

Cyclic Adenosine 5'-Diphosphate Ribose Analogs without a "Southern" Ribose Inhibit ADP-ribosyl Cyclase–Hydrolase CD38

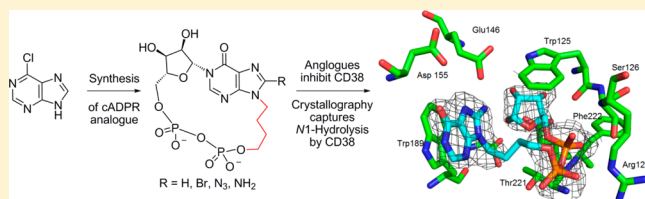
Joanna M. Swarbrick,[†] Richard Graeff,[‡] Hongmin Zhang,[‡] Mark P. Thomas,[†] Quan Hao,[‡] and Barry V. L. Potter*,[†]

[†]Wolfson Laboratory of Medicinal Chemistry, Department of Pharmacy and Pharmacology, University of Bath, Claverton Down, Bath, BA2 7AY, United Kingdom

[‡]Department of Physiology, University of Hong Kong, Hong Kong, China

Supporting Information

ABSTRACT: Cyclic adenosine 5'-diphosphate ribose (cADPR) analogs based on the cyclic inosine 5'-diphosphate ribose (cIDPR) template were synthesized by recently developed stereo- and regioselective N1-ribosylation. Replacing the base N9-ribose with a butyl chain generates inhibitors of cADPR hydrolysis by the human ADP-ribosyl cyclase CD38 catalytic domain (shCD38), illustrating the nonessential nature of the “southern” ribose for binding. Butyl substitution generally improves potency relative to the parent cIDPRs, and 8-amino-N9-butyl-cIDPR is comparable to the best noncovalent CD38 inhibitors to date ($IC_{50} = 3.3 \mu\text{M}$). Crystallographic analysis of the shCD38:8-amino-N9-butyl-cIDPR complex to a 2.05 Å resolution unexpectedly reveals an N1-hydrolyzed ligand in the active site, suggesting that it is the N6-imino form of cADPR that is hydrolyzed by CD38. While HPLC studies confirm ligand cleavage at very high protein concentrations, they indicate that hydrolysis does not occur under physiological concentrations. Taken together, these analogs confirm that the “northern” ribose is critical for CD38 activity and inhibition, provide new insight into the mechanism of cADPR hydrolysis by CD38, and may aid future inhibitor design.



INTRODUCTION

Cyclic adenosine 5'-diphosphate ribose (cADPR, 1, Figure 1)^{1,2} is synthesized in biological systems from nicotinamide adenine

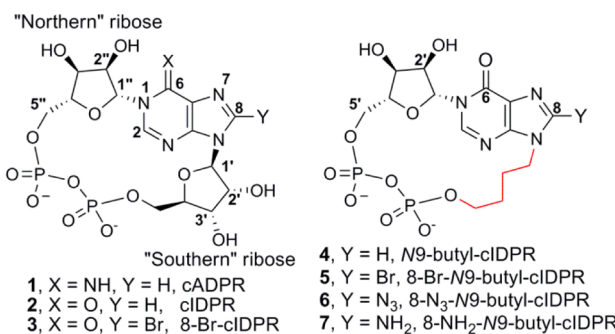


Figure 1. Structure of cADPR and N9-butyl analogs.

dinucleotide (NAD^+) by ADP-ribosyl cyclases (ADPRCs). It acts as a second messenger, mobilizing intracellular calcium.^{3–6}

In humans, formation of cADPR is catalyzed by the multifunctional transmembrane glycoprotein ADPRC CD38.⁷ CD38 also acts as an NAD^+ glycohydrolase (NADase) and as a cADPR hydrolase to generate adenosine 5'-diphosphate ribose (ADPR), another Ca^{2+} -releasing second messenger.^{8–10} Under acidic conditions, CD38 generates the most potent Ca^{2+} -releasing second messenger known to date, nicotinic acid

adenine dinucleotide phosphate (NAADP) from nicotinamide adenine dinucleotide phosphate (NADP).¹¹

CD38 knockout studies have revealed the importance of this pathway in a range of diseases. CD38 is a marker in AIDS progression¹² and a negative prognostic marker of chronic lymphocytic leukemia.¹³ It acts to regulate intracellular levels of NAD^+ , being implicated in energy homeostasis, signal transduction, and aging,^{14–16} and recently has been shown to be critical for social behavior in mice.¹⁷ The emerging role of CD38 in disease states is stimulating the search for modulators of activity for chemical biological studies and to provide structural clues for drug design and potential therapeutic candidates.¹⁸ To date, CD38 inhibitors fall broadly into two categories: mechanism-based covalent inhibitors that bind to the catalytic residue, and reversible, competitive, noncovalent inhibitors. Most are derived from NAD^+ and designed as inhibitors of the predominant NADase activity of CD38. Nicotinamide-based derivatives have demonstrated nanomolar inhibition of NADase activity by covalent modification of CD38¹⁹ and low millimolar activity when designed as membrane permeable analogs.²⁰ Competitive inhibitors are more diverse in structure, with a nonhydrolyzable NAD^+ analog reported ($IC_{50} \approx 150 \mu\text{M}$),²¹ flavonoids showing low micromolar inhibition²² and the development of a hit from

Received: July 10, 2014

Published: September 16, 2014

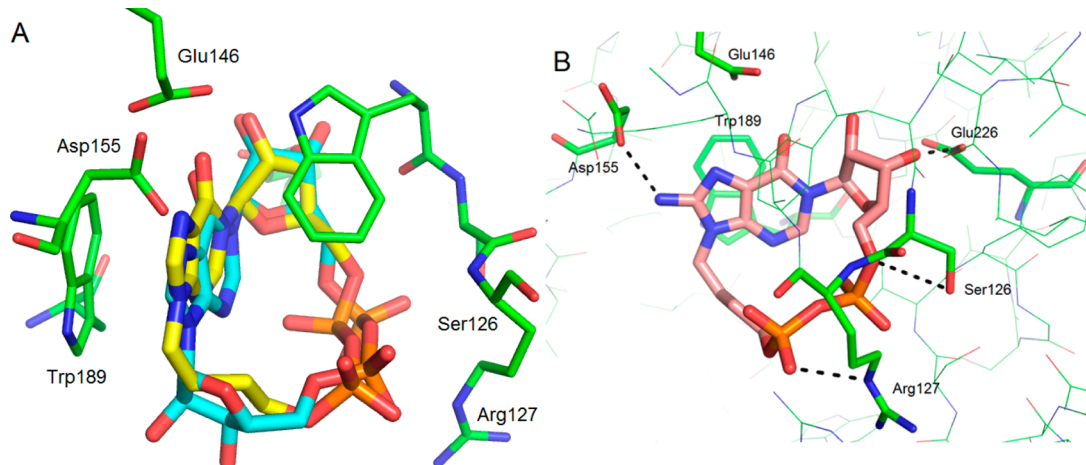


Figure 2. N9-Butyl-cIDPR docked into 2PGJ crystal structure. Comparison between 2PGJ crystal structure of N1-cIDPR (carbons in cyan) bound to shCD38 and (A) docked N9-butyl cIDPR 4 (carbons in yellow) showing overlap of their structures in the binding pocket; (B) interaction of 8-NH₂-N9-butyl cIDPR 7 (carbons in pink) with critical residues in the binding pocket and additional predicted H-bond to Asp155.

commercial libraries generating the most active reported noncovalent inhibitor to date ($IC_{50} = 4.7 \mu M$).²³

As both cADPR and ADPR are derived from a common intermediate,²⁴ we chose to design product-like inhibitors based on the cADPR structure to exploit inhibition of CD38 cADPR hydrolase activity. cADPR itself is unattractive for inhibitor design, since it is hydrolyzed at the N1 link in both neutral aqueous solution and under physiological conditions.^{25–27} More stable analogs have been accessed by one of two routes: either a chemoenzymatic route modeled on the biosynthesis of cADPR from NAD⁺ or by total chemical synthesis. We have previously reported a chemoenzymatic route to N1-cyclic inosine 5'-diphosphate ribose (cIDPR, 2) via its 8-bromo derivative (8-Br-cIDPR, 3, Figure 1).²⁸ Chemically and biologically stable, 2 and 3 both inhibit cADPR hydrolysis by the catalytic domain of CD38 (shCD38; IC_{50} of 276 and 158 μM , respectively). Furthermore, 2 acts as an agonist for Ca²⁺-release with almost equivalent potency to cADPR in permeabilized T-cells and 3 is a membrane permeant agonist.^{29,30}

Until recently, total synthetic approaches have required modification of the “northern” ribose to generate a more stable N1-link by introduction of a carbocyclic “northern” ribose,^{31–33} replacement of the “northern” ribose, or both ribose sugars, by an alkyl or ether bridge^{34,35} or by attaching the “northern” ribose to the base at C-2”.³⁶ We recently reported the use of modified Vorbrüggen conditions to effect stereo- and regiospecific introduction of an acetylated ribose at the N1-position of a protected inosine and demonstrated the utility of this method in the first total synthesis of 3.³⁷ This paves the way for further exploration of the structure–activity relationship (SAR) of cADPR, using the cIDPR template, with the opportunity to retain an intact “northern” ribose and without the structural limitations of using enzymatic cyclization.³⁸ We report here the synthesis of the first analogs in which the “southern” ribose is selectively replaced, the activity of these analogs as inhibitors of cADPR hydrolysis by shCD38, crystallography of the most potent inhibitor with shCD38, and HPLC studies to examine the ability of shCD38 to hydrolyze the cIDPR scaffold.

RESULTS AND DISCUSSION

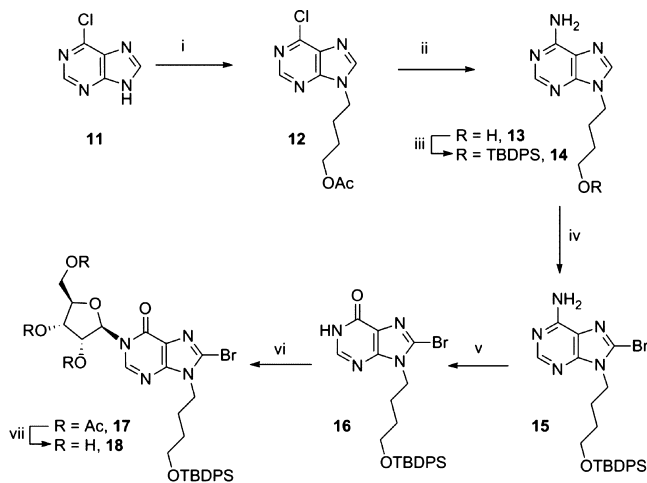
+ 既可以环化为 cADPR，也可以水解为 ADPR。^{39–41} 与 shCD38 结合的天然配体 2 (PDB 编号 2PGJ),⁴² 环状腺苷 5'-二磷酸核糖 (cADPcR, 3UHI),⁴³ 和 8-NH₂-cIDPR (3U4H) 建议一个关键作用于“北方”核糖，而“南方”核糖在开放面上被容纳。因此，我们设计了将“南方”核糖替换为 N9-烷基链 (N9-烷基-cIDPRs 4–7, 图 1) 的类似物，以探索是否需要 N9-核糖基链接来结合到 CD38 上。这些类似物可能具有更广泛的酸敏感性。⁴⁷

Molecular Modeling. 为了预测类似物 4–7 的结合模式，由于它们可能比 cADPR 更灵活，因此首先将其结合到 2PGJ 晶胞结构中，该结构为 shCD38 与 cIDPR 的复合物。结合并最小化后的构象几乎与 cIDPR (图 2A) 相同，表明这些类似物将模仿结合位点的的关键相互作用。蛋白最小化后几乎没有氨基酸残基移动。

结合的配体显示面对面堆叠在次黄嘌呤碱和 Trp189 之间。有一个预测的氢键从核糖 3'-OH^a 氢氧化基团到催化酸 (Glu226)，尽管 2'-OH 不那么靠近，且从 Ser126 和 Arg127 的侧链到磷酸根。7 的 8-氨基基团预测形成额外的氢键到 Asp155 的侧链。4 中的 N9-烷基链在结合口袋中几乎位于“南方”核糖的相同位置 (图 2B)。

Synthesis of N9-Butyl-cIDPR Analogs 4–7. 6-Chloropurine (11, Scheme 1) was alkylated with 4-chlorobutylacetate

Scheme 1. Synthesis of the N1-Ribosyl-N9-butyl-8-bromohypoxanthine Building Block^a



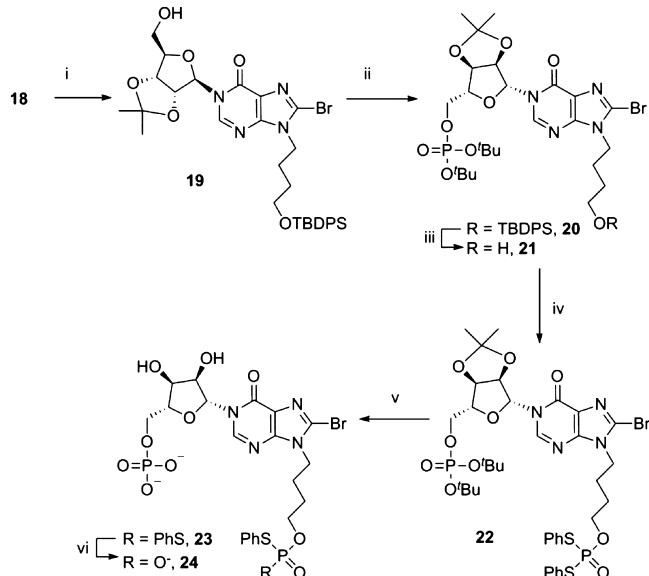
^aReagents: (i) DBU, 4-Cl-butyl-OAc, 77%; (ii) NH₃, MeOH, 96%; (iii) imidazole, TBDPS-Cl, 92%; (iv) (a) diisopropylamine, *n*-BuLi, (b) Br₂, 66%; (v) NaNO₂, AcOH (aq), 84%; (vi) (a) DBU, (b) tetraacetyl-D-ribose, TMSOTf, 86%; (vii) NH₃, MeOH, 98%.

in the presence of 1,8-diazabicyclo[5.4.0]undec-7-ene (DBU).⁴⁸ The desired major product, the N9-isomer 12, was obtained in high yield after separation from the minor N7-isomer. Treatment of 12 with methanolic ammonia at 80 °C efficiently effected both amination at the 6-position and deprotection of the N9-butyl acetyl ester to afford N9-hydroxybutyladenine 13.⁴⁹ The alkyl group was then reprotected as the TBDPS ether using *tert*-butyldiphenylsilyl chloride (TBDPS-Cl) and imidazole to give 14. Introduction of the 8-bromo substituent to 14 is crucial at this stage to promote the subsequent N1-ribosylation.³⁷ Attempted bromination of 14 using a solution of bromine in sodium hydrogen phosphate buffer and dioxane was not successful, and no reaction was observed. Similarly, treatment of 14 with *N*-bromosuccinimide or *N*-bromoacetamide afforded only starting material. Applying the conditions developed by Laufer et al.⁵⁰ for the 8-bromination of N9-methyl chloropurines, we first deprotonated 14 using lithium diisopropylamide (LDA), followed by addition of 1,2-dibromotetrachloroethane.⁵¹ On a small scale (100 mg) the desired 8-brominated product 15 was isolated in 67% yield. However, when this reaction was scaled up (2.5 g), an inseparable mixture of two products was obtained after column chromatography. Mass spectrometry (*m/z* = 480.1970 and 524.1476) containing characteristic ^{35/37}Cl and ^{79/81}Br isotope patterns confirmed this was both the 8-bromo and 8-chloro substituted products. It was only possible to recover the starting material by treating the mixture of products with Pd/C under an atmosphere of H₂. We therefore sought an alternative source of bromine that would avoid this complication and found that direct addition of Br₂ to deprotonated 14 generated 15 in 66% yield, with the remainder as starting material, which could be separated by column chromatography and reused. Treatment of 15 with excess sodium nitrite converted 8-bromoadenine 15 to 8-bromohypoxanthine 16, which was a suitable substrate for N1-ribosylation. Deprotonation of 16 with DBU followed by addition of tetraacetyl-D-ribose and trimethylsilyl triflate (TMSOTf)³⁷ afforded stereo- and regioselective N1-coupling to generate only the desired N1-ribosylated product 17 in high

yield. Deprotection of the three acetyl esters using methanolic ammonia generated triol 18.

The 2',3'-diol was reprotected as an isopropylidene ketal to afford 19, which allowed selective introduction of the first phosphate ester to the S'-OH by treatment of 19 with *N,N*-diisopropylbenzylphosphoramidite and 5-phenyl-1-*H*-tetrazole as activator, followed by oxidation of the intermediate phosphite with hydrogen peroxide and triethylamine (Scheme 2). The silyl ether of 20 was then removed under neutral

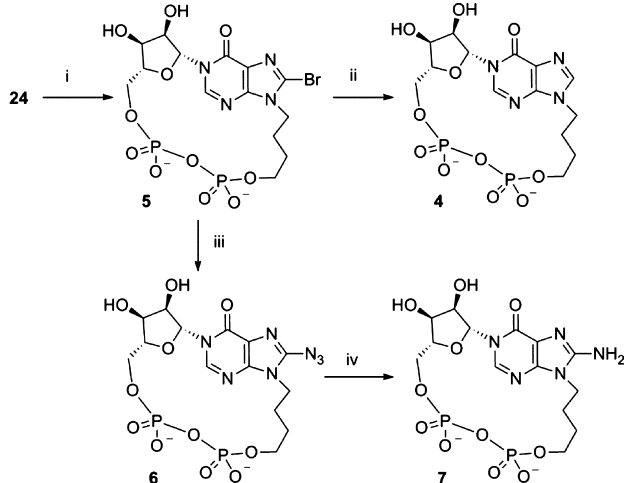
Scheme 2. Sequential Introduction of the Phosphate Esters^a



^aReagents: (i) pTsOH, H₃CC(OMe)₂CH₃, acetone, 100%; (ii) (a) (BuO)₂PN(Pr)₂, 5-Ph-1H-tetrazole, DCM; (b) H₂O₂, Et₃N, 80%; (iii) TBAF·3H₂O, AcOH, 100%; (iv) PSS, TPS-Cl, 5-Ph-1H-tetrazole, pyridine, 100%; (v) 50% TFA (aq), 100%; (vi) 0.1 M NaOH-dioxane.

conditions to reveal the hydroxyl group. The second protected phosphate ester was introduced by treatment of 21 with cyclohexylammonium S,S-diphenylphosphorodithioate (PSS), 2,4,6-triisopropylbenzenesulfonyl chloride (TPS-Cl), and 5-phenyl-1-*H*-tetrazole in pyridine under strictly dry conditions to generate the fully protected precursor for cyclization, 22. Sequential deprotection of the phosphates was carried out as previously described³⁷ using first 50% aqueous TFA to simultaneously remove the *tert*-butyl esters and the isopropylidene ketal, then 0.1 M sodium hydroxide in dioxane, to afford 24. The N9-butyl chain shows increased stability toward acidic conditions, compared to the natural “southern” ribose of cIDPR, which had initially suffered partial hydrolysis at the N9-glycosidic bond during deprotection of the isopropylidene acetals and *tert*-butyl phosphate esters.^{37,47} No degradation of the N9-butyl analogs was observed even over prolonged periods in 50% TFA at room temperature, since the ribose oxygen has been removed.

Cyclization of 24 was promoted using iodine and activated 3 Å molecular sieves in pyridine,³³ under very dilute conditions, to afford 5 (21% yield over two steps, Scheme 3). Because of the stability of our cIDPR-based analogs, modifications at the 8-position were possible after cyclization, which allowed us to generate three further analogs; 8-H, 8-N₃, and 8-NH₂. Subjecting 5 to an atmosphere of hydrogen with Pd/C catalysis generated the 8-H analog, N9-butyl-cIDPR (4). Treatment of 5

Scheme 3. Synthesis of N9-Butyl-cIDPR Analogs 4–7^a

^aReagents: (i) I₂, 3 Å molecular sieves, pyridine, 21%; (ii) H₂, Pd/C, NaHCO₃, EtOH-H₂O, 76%; (iii) TMSN₃, 57%; (iv) dithiothreitol, 0.05 M TEAB, 68%.

with NaN₃ in an attempt to generate the 8-N₃ analog **6** was not successful, despite conversion to the triethylamine salt or the free acid to improve the solubility of **5** in DMF. In each case, the DMF solution became cloudy over time as the sodium salt of the starting material was formed and became insoluble in the reaction media. However, upon treatment of the free acid form of **5** with TMSN₃ in DMF, no precipitation was observed and the clear solution was stirred at 70 °C for 16 h, becoming yellow in color as the reaction proceeded. The reaction progression was followed by RP-HPLC which clearly showed the shift in wavelength as the 8-bromo starting material ($\lambda_{\text{max}} = 255 \text{ nm}$) was converted into the 8-azido product [8-N₃-N9-butyl-cIDPR (**6**), $\lambda_{\text{max}} = 277 \text{ nm}$]. Treatment of **6** with dithiothreitol reduced the 8-azido substituent to an 8-amino group which gave 8-NH₂-N9-butyl-cIDPR (**7**).

Inhibition of CD38-Mediated cADPR Hydrolysis. The ability of the novel compounds **4–7** to inhibit shCD38-mediated hydrolysis of cADPR was assessed in a dose-response manner using a fluorimetric cycling assay.⁵² cIDPR (**2**) inhibits hydrolysis of cADPR with an IC₅₀ of 276 μM.⁴² The novel N9-butyl analogs **4–7** inhibit cADPR hydrolysis in a concentration-dependent manner, with half maximal inhibition in the low micromolar range (Figure 3 and Table 1). They are all more potent than **2**, showing an almost 100-fold increase in inhibition. The introduction of an 8-bromo substituent (**5**) gave a marginally improved inhibition (IC₅₀ = 27 μM) compared to the parent **4** (33 μM), which was then further improved by substitution to the 8-azido (**6**) or 8-amino (**7**) group (IC₅₀ of 6.4 and 3.3 μM, respectively). The trend of improved inhibition upon 8-H → 8-Br → 8-NH₂ substitution mimics that which was observed for the cIDPR series,⁴³ the 8-NH₂ derivative benefiting from an additional binding site interaction with Asp155. This suggests that the new analogs are binding similarly in the active site (vide infra). They are of comparable potency to the recently reported non-nucleoside and flavonoid NADase inhibitors.^{22,23} The improved inhibition of cADPR hydrolysis suggests that the “southern” ribose is not essential for activity.

The significant increase in potency by substitution of the “southern” ribose with a butyl chain may be a result of the

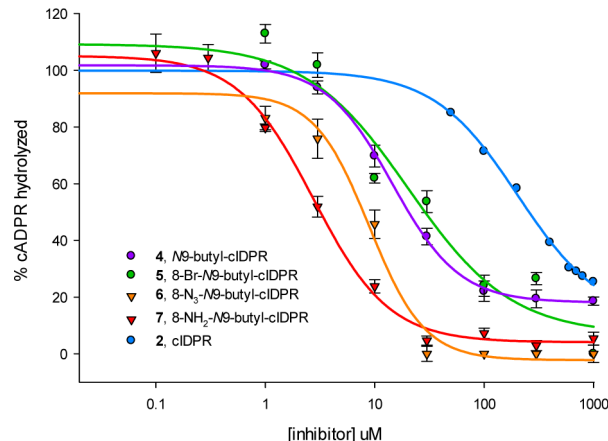


Figure 3. Inhibition of shCD38-mediated cADPR hydrolysis by analogs **4–7**.

Table 1. Half Maximal Values for Inhibition of shCD38-Mediated cADPR Hydrolysis by Novel Analogs **4–7 and Equivalent 8-Substituted cIDPRs**

cIDPR	IC ₅₀ (μM) ⁴³	N9-butyl-cIDPR	IC ₅₀ (μM)
8-H	2	4	33
8-Br	3	5	27
8-N ₃		6	6.4
8-NH ₂	56	7	3.3

increased flexibility afforded by an alkyl chain linker, compared to a ribose sugar. This might allow the ligand to align other key residues more favorably with their binding targets, resulting in a tighter affinity for CD38. Another factor may be the hydrophobic nature of the butyl chain, which may prefer to sit further into the binding pocket, in a less polar environment away from bulk solvent.

Structure of 8-NH₂-N9-butyl-cIDPR (7**) Complexed with Wild-Type CD38.** Preformed crystals of wild-type shCD38 were soaked with a cryoprotectant solution containing 5 mM 8-NH₂-N9-butyl-cIDPR (**7**). X-ray diffraction data were collected to a resolution of 2.05 Å. The structure was solved by the molecular replacement method revealing two molecules of CD38 in the asymmetric unit with a ligand present in each active site (Figure 4A). Previous crystallographic work⁴³ has generally shown occupancy of only one site by noncovalent inhibitors.

To our surprise, the electron density within each active site did not fit the cyclic compound **7**. However, hydrolysis at N1 to generate a linear compound, **7a**, gave a structure with a good fit (Figure 4B). After refinement, the complex clearly showed that the catalytic residue Glu226 was still hydrogen-bonded to the ribose. For molecule A, Glu226 H-bonds to the 1'- and 3'-OH of the ribose (both 2.7 Å), which has previously been observed in hydrolyzed intermediates or products.⁵³ In molecule B, Glu226 forms H-bonds with the 3'-OH (2.6 Å) and longer distance interactions with the 1'-OH and 2'-OH (3.3 and 3.5 Å). In both molecules, the 2'-OH interacts with an active site water molecule (Figure 4C). Addition of water to C-1' has occurred to generate the hydrolyzed product, and the -OH group is attached to the α-face of the ribose, as has been observed previously for NAD⁺ hydrolysis products captured by crystallization.^{53,54} Such observations are at odds with both the proposed ionic or covalent hydrolysis mechanisms, which predict a predominantly or entirely β-product, respectively.⁵⁵

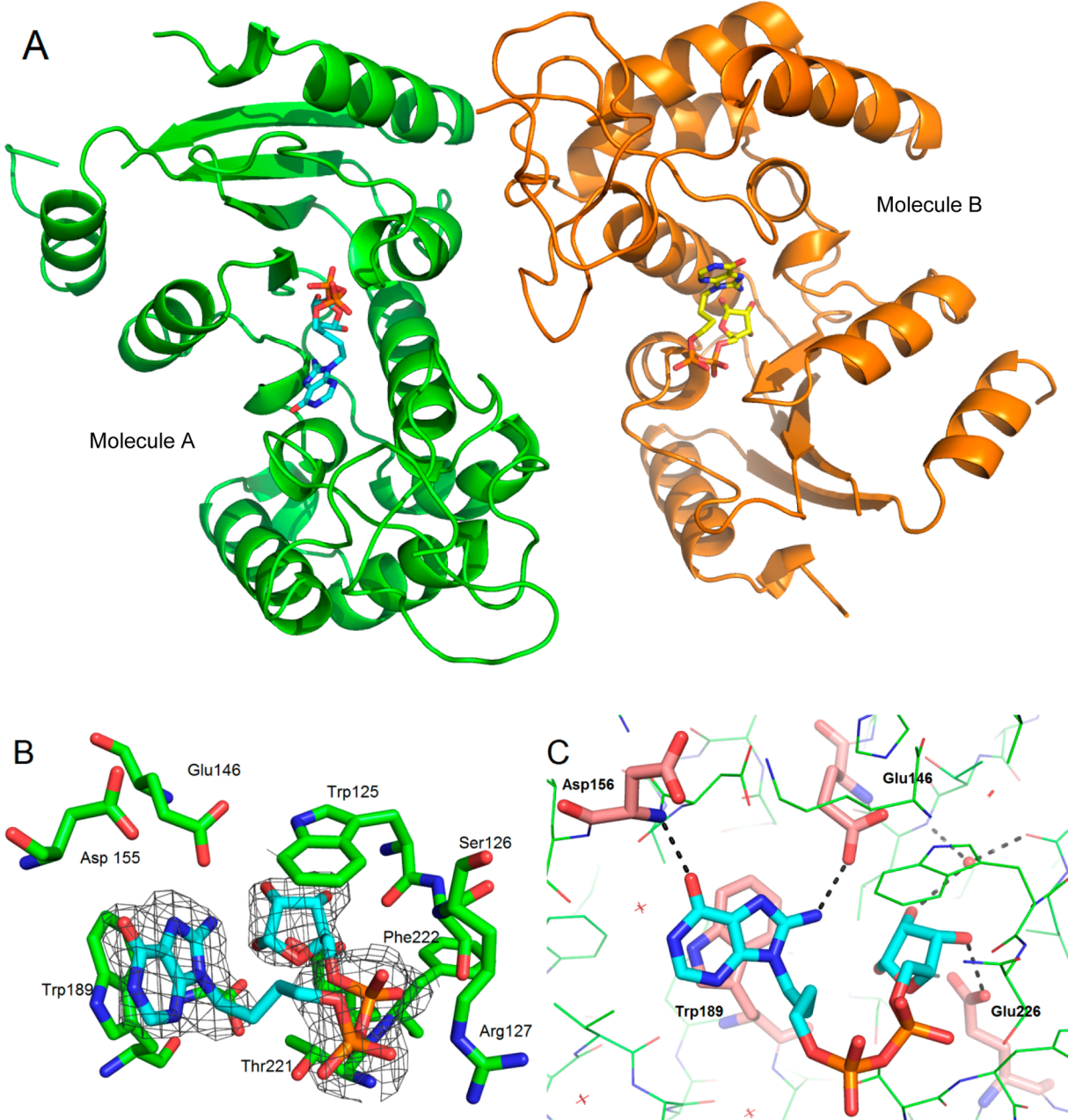


Figure 4. Crystal structure of PDB code 4TMF. (A) Ligand (shown as sticks) occupies each active site. (B) The electron density fits of a hydrolyzed ligand (carbons in cyan, key residues that interact with the ligand in the binding site shown as green sticks). (C) H-bonds (shown as black dotted lines) are formed between the rotated hypoxanthine base and both Glu146 and the backbone nitrogen of Asp156. Interacting residues are shown as pink sticks, and other residues are shown as green lines. The interacting binding site water is shown as a red sphere, and the other waters as red crosses.

Notably, the hydrolyzed ligand still occupies the catalytic site in the same manner as the cADPR, except that the hypoxanthine base has rotated in the binding pocket after hydrolysis. While maintaining the stacking interaction with Trp189, it has also formed new hydrogen bonds with Glu146 and Asp156 via its 8-NH₂ and 6-O substituents, respectively (Figure 4C). It is unusual to capture this snapshot of the ligand directly after hydrolysis, before diffusion out of the binding site. Previously reported crystal structures of the hydrolysis products of N7-cGDPR and cADPR, GDPR and ADPR, respectively, have also captured products that were not bound in a conformation directly resulting from hydrolysis.⁵³

Proposed Mechanism of Hydrolysis by CD38. Finding a hydrolyzed ligand in the active site of CD38 was unexpected, as the cIDPR template has previously been considered “non-hydrolyzable”.⁴² The absence of a partial positive charge at N1, compared to that in the N6-amino form of cADPR, was thought to contribute to this stability (Figure 5).

However, a mechanism in which the anomeric oxygen assists in breaking the N1-link could still be envisaged (Scheme 4). This would be without prejudice as to whether the role of Glu226 is to capture the resulting oxonium ion formally or interact with it as an ion pair before insertion of water to generate the final linear product. Examination of the crystal structures 2PGJ and 3U4H suggests that both binding sites

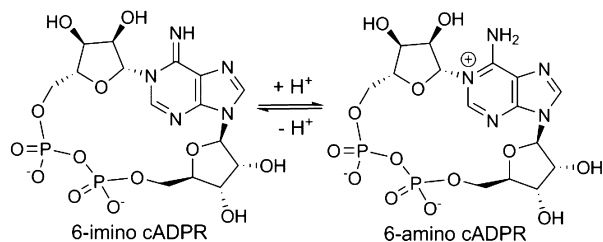


Figure 5. cADPR has a partial positive charge at N1.

contain two water molecules close to the N1-link of the cyclic ligand. One of these waters forms H-bonds to Leu123, Leu145, and the ribose 2'-OH that is consistent with other reported CD38 crystal structures.⁵⁴ Notably, in the 3U4H crystal with 8-NH₂-cIDPR, the remaining water molecule lies within 3 Å of the hypoxanthine carbonyl group. This water is not observed in the complex of the hydrolyzed ligand **7a** (PDB code 4TMF); thus, we postulate that donation of a proton from this water molecule could be enzyme-assisted in the active site. Further examination reveals a proximal histidine residue (His133) that may potentially contribute to overall catalysis (Figure 6).

For the corresponding cADPR ligand to be hydrolyzed via such a mechanism would require the ligand to be present in the N6-imino form. Indeed, an earlier report indicated that cADPR exists in two forms, the N6-imino and N6-amino, the latter with a pK_a of 8.3.⁵⁶ Although at physiological pH the amino form will be predominant, the active form for Ca²⁺ release remains unresolved and crystallization of cADPR originally suggested that the C6–N6 bond displayed double bond characteristics (length 1.33 Å, cf. 1.47 Å expected for an amino group) with only one hydrogen atom bound to N6.² This is somewhat surprising given that the molecule was crystallized as its free acid, presumably well below pH 8.3. The C6–N6 bond length

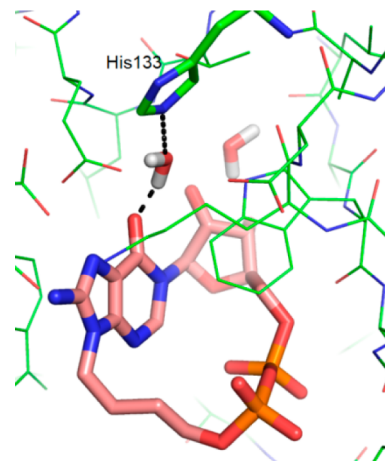
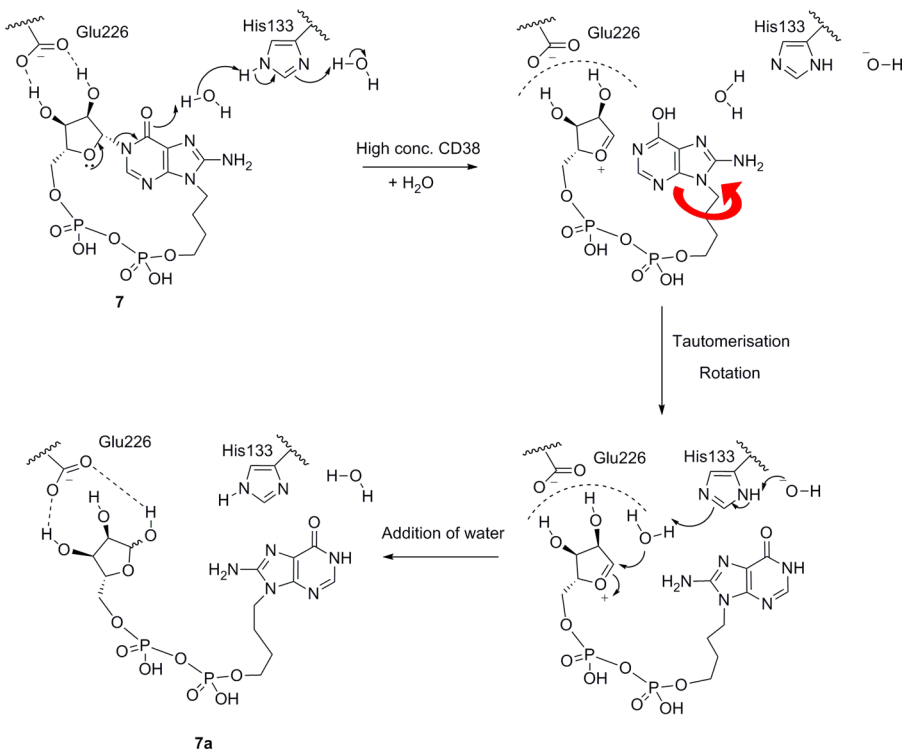


Figure 6. Docking of 8-NH₂-N9-butyl-cIDPR (**7**) into 3U4H after removal of ligand (ligand carbons in pink sticks, protein carbons in green).

in the cADPcR-shCD38 complex,⁴³ the only cocrystal structure of a cyclic ligand with a starting C6-substituent in the amino form yet determined, measures 1.35 Å, also suggesting substantial double bond character. The authors measured the pK_a of the N6-amino dissociation in this case as 8.9.²⁶ However, cADPcR is a completely nonhydrolyzable ligand due to the absence of the ribose oxygen. Since crystallization of cADPR itself with shCD38 is not possible because of its very rapid hydrolysis, it has been impossible to capture directly the intermediates in this process. Previously, the surrogate substrate NGD⁺ revealed the role of Glu226 in activating and stabilizing the intermediate precursor for hydrolysis or cyclization.⁵³ We originally showed that cIDPR, as expected, has no ionization between 6.8 and 10.9²⁸ and it is not likely that **7** will be any

Scheme 4. Proposed Mechanism for Hydrolysis of **7** by a High Concentration of shCD38



different. Thus, since it is unlikely that cIDPR or any related analog will exist in the 6-phenolic form at the pH used with shCD38 (*vide infra*) and the enzyme would not adopt a different mechanism to hydrolyze an analog vs cADPR itself, we can conclude that the complex of **7a** with shCD38 provides the first evidence that CD38 can bind cADPR in the N6-imino form. This could have future implications for inhibitor design. We clearly cannot comment upon the ability of CD38 to bind the N6-amino form of cADPR.

Study of Ligand Hydrolysis by CD38. Following the discovery of hydrolyzed ligand **7a** in the crystal complex, it was important to determine whether it is the cyclic or the hydrolyzed linear compound that inhibits hydrolysis of cADPR by shCD38. Incubation of **7** (1 mM final concentration) with 4 mg/mL shCD38 was monitored using RP-HPLC. The peak corresponding to **7** ($t_R = 9.1$ min) reduced in intensity over time, alongside the appearance of a new peak ($t_R = 10.6$ min), which was characteristic of an ADPR analog (see Supporting Information, Figure S1). The rate of conversion depended on the concentration of CD38 present in solution (Figure S2), and no change in the original peak was observed in a parallel control experiment containing no shCD38 (data not shown). Novel analogs **4**, **5** and cIDPR (**2**) were also analyzed in this way (Figure 7). Surprisingly, we

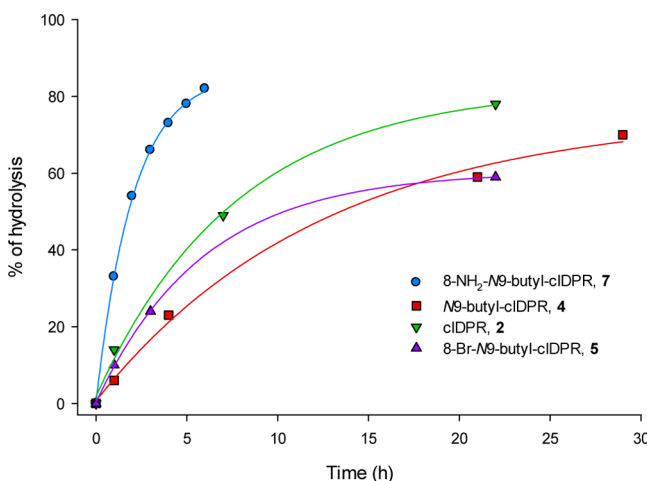


Figure 7. Hydrolysis of analogs **4**, **5**, **7**, and cIDPR (**2**) over time with shCD38 (4 mg/mL).

found that all the compounds, including cIDPR, are hydrolyzed by the enzyme at 4 mg/mL but at a slower rate than **7**. The increased rate of hydrolysis of **7** could conceivably be promoted by the additional hydrogen bond generated between the 8-NH₂ substituent and Asp155 promoting elongation of the N1-bond toward the transition state. This faster hydrolysis of **7** under these conditions (50% hydrolysis for **7** at $T = 105$ min and for cIDPR at $T = 420$ min), also reinforced by the extra interaction afforded by the 8-amino group after cleavage, perhaps explains why the hydrolyzed ligand **7a** is captured in the 8-NH₂-N9-butyl-cIDPR:CD38 complex, but a cyclic ligand is observed in the previously reported cIDPR:CD38 complex 2PGJ.⁴²

These conditions are representative of crystallization concentrations of shCD38 (10 mg/mL) and are 10,000-fold more concentrated than those used in the enzyme assay (1 μ g/mL). Therefore, further HPLC experiments were carried out using shCD38 concentrations of 1 μ g/mL and either cIDPR or **7** to observe the effect of CD38 under conditions that reflect

the enzyme assay (Supporting Information, Figure S3). Under these conditions the ligand is not hydrolyzed, confirming that the inhibition observed in the CD38 assay is a consequence of the cyclic compounds, not their hydrolyzed counterparts.

CONCLUSION

Two of the analogs developed in this study are potent (≤ 10 μ M) inhibitors of cADPR hydrolysis by CD38. Analogs **4**–**7** illustrate that the “southern” ribose can be modified to considerably improve inhibitory activity of CD38 mediated cADPR hydrolysis. This agrees with modeling predictions based on the shCD38-ligand crystal structure complex interactions and confirms that the “northern” ribose and base are key features for the interaction of cADPR analogs with the CD38 binding pocket. The investigation of SAR in this region in isolation was not possible prior to development of a method for N1-ribosylation. This method thus opens up new avenues and the potential to introduce desirable characteristics, such as membrane permeability, into cADPR analogs by modifications in this region, without loss of activity at CD38. Crystallization of 8-NH₂-N9-butyl-cIDPR with shCD38 revealed that the cIDPR scaffold can unexpectedly be hydrolyzed at high concentrations of shCD38, resulting in a cocrystal structure with linear 8-NH₂-N9-butyl-IDPR (**7a**) in the active site. Hydrolysis of the hypoxanthine-linked scaffold offers new insight into the mechanism by which CD38 hydrolyzes cADPR to ADPR and suggests for the first time that the imino form is active in this process. However, HPLC studies suggest that hydrolysis would not occur under assay or physiologically relevant concentrations. Thus, this observation does not detract from the established use of cIDPR or its derivatives as either pharmacological tools or as nonhydrolyzable templates for future CD38 inhibitor design or indeed of 8-Br-cIDPR (**3**)³⁰ as a stable membrane permeant agonist of Ca²⁺ release.

EXPERIMENTAL SECTION

General. All reagents and solvents were of commercial quality and were used without further purification, unless described otherwise. Unless otherwise stated, all reactions were carried out under an inert atmosphere of argon. ¹H, ¹³C, and ³¹P NMR spectra were collected on a Varian Mercury 400 MHz or Bruker Avance III 500 MHz spectrometer. All ¹H and ¹³C NMR assignments are based on gCOSY, gHMBC, gHSQC, and DEPT-135 experiments. Abbreviations for splitting patterns are as follows: b, broad; s, singlet; d, doublet; t, triplet; m, multiplet. Coupling constants are given in hertz (Hz). High resolution time-of-flight mass spectra were obtained on a Bruker Daltonics micrOTOF mass spectrometer using electrospray ionization (ESI). The purity of new tested compounds was determined to be $\geq 95\%$ by analytical HPLC. Analytical HPLC analyses were carried out on a Waters 2695 Alliance module equipped with a Waters 2996 photodiode array detector (210–350 nm). The chromatographic system consisted of a a Hichrom Guard column for HPLC and a Phenomenex Syngi 4 μ m MAX-RP 80A column (150 mm \times 4.60 mm), with elution at 1 mL/min with the following ion-pair buffer: 0.17% (m/v) cetrimide and 45% (v/v) phosphate buffer (pH 6.4) in MeOH. Synthetic phosphates were assayed and quantified by the Ames phosphate test.⁵⁷

6-Chloro-9-(4-acetoxybutyl)purine (12).⁴⁸ To 6-chloropurine **11** (2.50 g, 16.2 mmol) and DBU (2.91 mL, 19.4 mmol) in DMF (22 mL) was added 4-chlorobutylacetate (4.54 mL, 32.3 mmol). After the mixture was stirred at 60 °C for 14 h, the DMF was removed under reduced pressure, and the residue was purified by column chromatography on silica gel, eluting with PE/EtOAc (1:0 \rightarrow 0:1 v/v) to afford the title compound (3.07 g, 71%) as a colorless oil. $R_f = 0.61$ (DCM/MeOH 9:1 v/v); ¹H NMR (400 MHz, MeOD) δ 8.78 (s,

1H), 8.16 (s, 1H), 4.37 (t, 2H, J = 7.2, CH₂), 4.15 (t, 2H, J = 6.4, CH₂), 2.08–2.04 (m, 5H, CH₂ and OAc), 1.74–1.67 (m, 2H, CH₂) ppm.

9-(4-Hydroxybutyl)adenine (13).⁴⁹ A solution of **12** (3.00 g, 11.2 mmol) in MeOH (7 mL) was cooled to 0 °C and saturated with NH₃ (g), then stirred for 14 h at 80 °C. On cooling, a white solid precipitated, which was collected by filtration and air-dried to afford the title compound (2.22 g, 96%). R_f = 0.17 (DCM/MeOH 9:1 v/v); ¹H NMR (400 MHz, MeOD) δ 8.23 (s, 1H), 8.16 (s, 1H), 4.30 (t, 2H, J = 7.2, CH₂), 3.61 (t, 2H, J = 6.4, CH₂), 2.03–1.96 (m, 2H, CH₂), 1.61–1.54 (m, 2H, CH₂) ppm; HRMS (ESI⁺) calcd for C₉H₁₄N₅O₁ 208.1193 [(M + H)⁺], found 208.1195.

9-(4-tert-Butyldiphenylsilylbutyl)adenine (14). To **13** (2.00 g, 9.65 mmol) in DMF (20 mL) were added imidazole (1.71 g, 25.09 mmol) and TBDPS-Cl (3.25 mL, 12.55 mmol). After 14 h at rt, all solvents were evaporated and the residue was purified by column chromatography on silica gel, eluting with DCM/acetone (1:0 → 0:1 v/v) to afford the title compound (3.96 g, 92%) as a white solid. R_f = 0.42 (DCM/acetone 1:3 v/v); ¹H NMR (400 MHz, CDCl₃) δ 8.21 (s, 1H), 8.09 (s, 1H), 7.62–7.60 (m, 4H), 7.43–7.35 (m, 6H), 4.26 (t, 2H, J = 7.0, CH₂), 3.71 (t, 2H, J = 6.2, CH₂), 2.05–1.97 (m, 2H, CH₂), 1.58–1.52 (m, 2H, CH₂), 1.01 (s, 9H) ppm; ¹³C NMR (100 MHz, CDCl₃) δ 155.3, 153.0, 150.2, 140.5, 135.5 (4C), 133.7 (2C), 129.7 (2C), 127.7 (4C), 119.8, 63.0, 43.8, 29.5, 26.9 (3C), 26.7, 19.2 ppm; HRMS (ESI⁺) calcd for C₂₅H₃₂N₅OSi 446.2371 [(M + H)⁺], found 446.2377.

9-(4-tert-Butyldiphenylsilylbutyl)-8-bromoadenine (15). To diisopropylamine (4.67 mL, 33.32 mmol) in THF (20 mL) at -78 °C was added n-butyllithium (21.2 mL, 1.6 M solution, 33.97 mmol), dropwise. After 1 h, a solution of **14** (2.97 g, 6.66 mmol) in THF (25 mL) was added dropwise and stirring continued for a further 1 h. Br₂ (2.04 mL, 39.96 mmol) was added dropwise and the solution allowed to warm to rt over 4 h. The reaction was quenched by addition of NH₄ (aq, 2 mL), and all solvents were evaporated. The residue was taken up in DCM/H₂O (1:1 v/v, 100 mL) and the organic layer separated, washed with brine, dried (Na₂SO₄), and evaporated to dryness. The crude material was purified by column chromatography on silica gel, eluting with DCM/acetone (1:0 → 0:1 v/v) to afford the title compound (2.18 g, 62%) as an amorphous cream solid. R_f = 0.61 (DCM/acetone 1:1 v/v); ¹H NMR (400 MHz, MeOD) δ 8.31 (s, 1H, H-2), 7.64–7.62 (m, 4H), 7.40–7.33 (m, 6H), 5.85 (bs, 2H, NH₂), 4.22 (t, 2H, J = 7.4, CH₂), 3.70 (t, 2H, J = 6.1, CH₂), 2.00–1.93 (m, 2H, CH₂), 1.62–1.55 (m, 2H, CH₂), 1.03 (s, 9H) ppm; ¹³C NMR (100 MHz, CDCl₃) δ 154.2, 153.0, 151.3, 135.5 (4C), 133.7 (2C), 129.6 (2C), 127.8 (4C), 127.3, 119.9, 63.0, 44.4, 29.4, 26.8 (3C), 26.1, 19.1 ppm; HRMS (ESI⁺) calcd for C₂₅H₃₁N₅OSi⁷⁹Br 524.1476 [(M + H)⁺], found 524.1473, calcd for C₂₅H₃₁N₅OSi⁸¹Br 526.1455 [(M + H)⁺], found 526.1462.

9-(4-tert-Butyldiphenylsilylbutyl)-8-bromohypoxanthine (16). To **15** (4.13 g, 7.87 mmol) in AcOH/H₂O (20:3 v/v, 138 mL) was added NaNO₂ (6.52 g, 94.48 mmol) in one portion. After 48 h, all solvents were evaporated and EtOH (100 mL) was added and evaporated to dryness. The residue was taken up in CHCl₃ and washed with H₂O, then NaHCO₃ (aq sat.) to pH 7. The organic layer was washed with brine, dried (Na₂SO₄), and evaporated to dryness. The crude material was purified by column chromatography on silica gel, eluting with PE/EtOAc (1:0 → 0:1 v/v) to afford the title compound (3.49 g, 84%) as a cream foam. R_f = 0.37 (PE/EtOAc 1:3 v/v); ¹H NMR (400 MHz, CDCl₃) δ 13.07 (bs, 1H, NH), 8.16 (s, 1H, 2H), 7.65–7.63 (m, 4H), 7.41–7.34 (m, 6H), 4.21 (t, 2H, J = 7.3, CH₂), 3.71 (t, 2H, J = 6.0, CH₂), 1.96 (tt, 2H, J = 7.4, 7.3, CH₂), 1.58 (tt, 2H, J = 6.5, 6.0, CH₂), 1.04 (s, 9H) ppm; ¹³C NMR (100 MHz, CDCl₃) δ 158.0, 150.6, 145.5, 135.6 (4C), 133.8 (2C), 129.7 (2C), 127.7 (4C), 126.3, 124.8, 63.0, 44.8, 29.4, 26.9 (3C), 26.2, 19.2 ppm; HRMS (ESI⁺) calcd for C₂₅H₃₀N₄O₂Si⁷⁹Br 525.1316 [(M + H)⁺], found 525.1319, calcd for C₂₅H₃₀N₄O₂Si⁸¹Br 527.1295 [(M + H)⁺], found 527.1301.

N1-(2',3',5'-Tri-O-acetyl-β-D-ribofuranosyl)-N9-[4-(tert-butylidiphenylsilyl)oxybutyl]-8-bromohypoxanthine (17). Intermediate **16** (400 mg, 0.761 mmol) was taken up in DCM (4.0 mL),

and DBU (341 μ L, 2.283 mmol) was added. After 30 min, 1,2,3,5-tetra-O-acetyl-β-D-ribofuranose (266 mg, 0.837 mmol) was added and the solution cooled to -78 °C. Trimethylsilyl trifluoromethanesulfonate (551 μ L, 3.044 mmol) was added dropwise and the solution stirred for a further 45 min before warming to rt. After 1 h, NaHCO₃ (sat. aq.) was added and the crude material extracted into DCM (\times 3). The combined organic fractions were dried (Na₂SO₄), and solvent was evaporated under reduced pressure. The residue was purified by column chromatography on silica gel, eluting with PE/EtOAc (1:0 → 1:0 v/v) to afford the title compound (203 mg, 90%) as a colorless glass. R_f = 0.69 (PE/EtOAc 1:3 v/v); ¹H NMR (400 MHz, CDCl₃) δ 8.14 (s, 1H, 2H), 7.63 (dd, 4H, J = 7.8, 1.5), 7.40–7.34 (m, 6H) (10 × Ar-H), 6.39 (d, 1H, J = 4.6, H-1'), 5.47 (dd, 1H, J = 5.8, 4.6, H-2'), 5.44 (dd, 1H, J = 5.8, 4.5, H-3'), 4.42–4.38 (m, 3H, H-4' and both H-5'), 4.17 (t, 2H, J = 7.3, CH₂), 3.70 (t, 2H, J = 6.0, CH₂), 2.13 (s, 3H), 2.11 (s, 3H), 2.07 (s, 3H) (3 × OAc), 1.96–1.92 (m, 2H, CH₂), 1.58–1.54 (m, 2H, CH₂), 1.03 (s, 9H) ppm; ¹³C NMR (100 MHz, CDCl₃) δ 170.2, 169.58, 169.57, 154.8, 148.7, 144.1, 135.5 (4C), 133.7 (2C), 129.7 (2C), 127.7 (4C), 126.1, 124.1, 87.3, 80.3, 74.2, 70.3, 63.0, 62.9, 44.7, 29.4, 26.9 (3C), 26.3, 20.8, 20.5, 20.4 19.2 ppm; HRMS (ESI⁺) calcd for C₃₆H₄₄N₄O₉Si⁷⁹Br 783.2055 [(M + H)⁺], found 783.2046, calcd for C₃₆H₄₄N₄O₉Si⁸¹Br 785.2035 [(M + H)⁺], found 785.2042.

N1-(β-D-Ribofuranosyl)-N9-[4-(tert-butylidiphenylsilyl)oxybutyl]-8-bromohypoxanthine (18). Intermediate **17** (600 mg, 0.766 mmol) was taken up in MeOH (6 mL) in a pressure tube. The solution was saturated with NH₃ (g) at 0 °C, then stirred at rt for 12 h. The solvent was evaporated and the residue purified by column chromatography on silica gel, eluting with PE/EtOAc (1:0 → 1:0 v/v) to afford the title compound (492 mg, 98%) as a white amorphous solid. R_f = 0.35 (DCM/acetone 1:1 v/v); ¹H NMR (500 MHz, MeOD) δ 8.79 (s, 1H, H-2), 7.62–7.60 (m, 4H), 7.42–7.35 (m, 6H) (10 × Ar-H), 6.22 (d, 1H, J = 3.1, H-1'), 4.32–4.28 (m, 2H, H-2', H-3'), 4.23 (t, 2H, J = 7.1, CH₂), 4.13 (ddd, 1H, J = 5.5, 2.9, 2.5, H-4'), 3.98 (dd, 1H, J = 12.3, 2.5, H-5a'), 3.83 (dd, 1H, J = 12.3, 2.9, H-5b'), 3.70 (t, 2H, J = 6.0, CH₂), 1.98–1.92 (m, 2H, CH₂), 1.55–1.49 (m, 2H, CH₂), 1.02 (s, 9H) ppm; ¹³C NMR (125 MHz, MeOD) δ 156.9, 150.5, 147.1, 136.6 (4C), 134.8 (2C), 130.9 (2C), 128.8 (4C), 127.7, 124.6, 91.5, 86.2, 76.9, 70.6, 64.1, 61.7, 45.7, 30.4, 27.4 (3C), 27.1, 19.9 ppm; HRMS (ESI⁺) calcd for C₃₀H₃₈N₄O₆Si⁷⁹Br 657.1739 [(M + H)⁺], found 657.1747, calcd for C₃₀H₃₈N₄O₆Si⁸¹Br 659.1718 [(M + H)⁺], found 659.1729.

N1-(2',3'-O-Isopropylidine-β-D-ribofuranosyl)-N9-[4-(tert-butylidiphenylsilyl)oxybutyl]-8-bromohypoxanthine (19). To **18** (430 mg, 0.634 mmol) in acetone/2,2-dimethoxypropane (5 mL, 4:1 v/v) was added p-TsOH (124 mg, 0.634 mmol). After 30 min, DCM and NaHCO₃ (sat. aq) were added, the organic layer was dried (Na₂SO₄), and all solvents were evaporated. The residue was taken up in MeOH (2 mL), and Dowex 50WX8 H⁺ resin (50 mg) was added. After 30 min the resin was removed by filtration under gravity and the solvent evaporated to obtain the title compound (455 mg, 100%) as a colorless glass. R_f = 0.63 (PE/EtOAc 1:3 v/v); ¹H NMR (400 MHz, CDCl₃) δ 7.87 (s, 1H, H-2), 7.55 (dd, 4H, J = 5.9, 1.5), 7.35–7.26 (m, 6H) (10 × Ar-H), 5.62 (d, 1H, J = 2.8, H-1'), 5.23 (dd, 1H, J = 6.5, 2.8, H-2'), 5.08 (dd, 1H, J = 6.5, 3.6, H-3'), 4.28 (dd, 1H, J = 3.6, 2.4, H-4'), 4.09 (t, 2H, J = 7.3, CH₂), 3.85 (dd, 1H, J = 12.2, 2.4, H-5a'), 3.75 (bd, 1H, J = 12.2, H-5b'), 3.61 (t, 2H, J = 6.0, CH₂), 1.89–1.82 (m, 2H, CH₂), 1.52 (s, 3H) 1.50–1.45 (m, 2H, CH₂), 1.28 (s, 3H), 1.02 (s, 9H) ppm; ¹³C NMR (100 MHz, CDCl₃) δ 155.3, 149.1, 146.5, 135.5 (4C), 133.6 (2C), 129.6 (2C), 127.6 (4C), 126.5, 124.8, 114.2, 97.1, 88.1, 83.5, 80.6, 62.8, 62.8 (2C), 44.7, 29.2, 27.3, 26.8 (3C), 26.1, 25.2, 19.1 ppm; HRMS (ESI⁺) calcd for C₃₃H₄₂N₄O₆Si⁷⁹Br 697.2052 [(M + H)⁺], found 697.2072, calcd for C₃₃H₄₂N₄O₆Si⁸¹Br 699.2031 [(M + H)⁺], found 699.2032.

N1-[2',3'-O-Isopropylidine-5'-O-(di-tert-butyl)phosphoryl-β-D-ribofuranosyl]-N9-[4-(tert-butylidiphenylsilyl)oxybutyl]-8-bromohypoxanthine (20). To a solution of **19** (350 mg, 0.502 mmol) in DCM (2.8 mL) was added 5-phenyl-1-H-tetrazole (147 mg, 1.003 mmol) and N,N-diisopropylbutylphosphoramidite (238 μ L, 0.753 mmol). After 2 h, the solution was cooled to 0 °C and Et₃N (419 μ L, 3.012 mmol) and H₂O₂ (138 μ L, 1.255 mmol) were added.

The solution was allowed to warm to rt and stirred for a further 2 h, after which DCM (20 mL) and H₂O were added. The organic layer was washed with NaHCO₃ (sat. aq), then brine, dried (Na₂SO₄), and evaporated to dryness. The residue was purified by column chromatography on silica gel, eluting with PE/EtOAc (1:0 → 1:0 v/v), where both solvents contained 0.5% v/v pyridine, to afford the title compound (356 mg, 80%) as a colorless glass. *R*_f = 0.43 (PE/EtOAc 1:3 v/v); ¹H NMR (400 MHz, CDCl₃) δ 8.02 (s, 1H, H-2), 7.63–7.60 (m, 4H), 7.40–7.32 (m, 6H) (10 × Ar-H), 5.97 (d, 1H, *J* = 1.8, H-1'), 5.08 (dd, 1H, *J* = 6.4, 1.8, H-2'), 4.99 (dd, 1H, *J* = 6.4, 3.9, H-3'), 4.41 (dd, 1H, *J* = 9.6, 4.3, H-4'), 4.27–4.13 (m, 4H, both H-5' and CH₂), 3.67 (t, 2H, *J* = 6.0, CH₂), 1.93–1.89 (m, 2H, CH₂), 1.57 (s, 3H), 1.55–1.44 (m, 2H, CH₂), 1.448 (s, 9H), 1.447 (s, 9H), 1.33 (s, 3H), 1.02 (s, 9H) ppm; ¹³C NMR (100 MHz, CDCl₃) δ 153.0, 147.2, 144.1, 133.7 (4C), 131.9 (2C), 127.8 (2C), 125.8 (4C), 124.2, 122.7, 112.5, 92.5, 85.1 (d, *J* = 7.9), 83.2, 80.9 (d, 2C, *J* = 7.2), 79.7, 64.7 (d, *J* = 6.2), 61.1, 42.8, 28.0 (d, 3C, *J* = 2.8), 27.9 (d, 3C, *J* = 2.9), 27.5, 25.3, 25.0 (3C), 24.4, 23.5, 17.3 ppm; ³¹P NMR (162 MHz, ¹H decoupled, CDCl₃) δ -10.2 ppm; HRMS (ESI⁺) calcd for C₄₁H₅₈N₄O₉PSi⁷⁹BrNa 911.2786 [(M + H)⁺], found 911.2762, calcd for C₄₁H₅₈N₄O₉PSi⁸¹BrNa 913.2766 [(M + H)⁺], found 913.2763.

N1-[2',3'-O-Isopropylidine-5'-O-(di-tert-butyl)phosphoryl-β-D-ribofuranosyl]-N9-(4-hydroxybutyl)-8-bromohypoxanthine (21). Acetic acid (12 μL, 0.213 mmol) and TBAF·3H₂O (64 mg, 0.203 mmol) were stirred in DMF (0.5 mL) for 30 min, after which the solution was cooled to 0 °C and 20 (60 mg, 0.068 mmol) in DMF (0.5 mL) added. The resulting solution was allowed to warm to rt and stirred for a further 4 h. The solution was diluted with ether, and NaHCO₃ (sat. aq) and NH₃Cl (sat. aq) were added. The organic layer was separated and the aqueous layer extracted with ether (×3). The combined organic layers were dried (Na₂SO₄), evaporated to dryness and the residue was purified by column chromatography on silica gel, eluting with DCM/acetone (1:0 → 1:0 v/v) to afford the title compound (44 mg, 100%) as a colorless glass. *R*_f = 0.47 (DCM/acetone 1:1 v/v); ¹H NMR (400 MHz, CDCl₃) δ 8.06 (s, 1H, H-2), 5.98 (d, 1H, *J* = 1.8, H-1'), 5.05 (dd, 1H, *J* = 6.4, 1.8, H-2'), 4.96 (dd, 1H, *J* = 6.4, 3.9, H-3'), 4.39 (app. dd, 1H, *J* = 9.0, 4.5, H-4'), 4.25–4.11 (m, 4H, both H-5' and CH₂), 3.65 (t, 2H, *J* = 6.3, CH₂), 2.34 (bs, 1H, OH), 1.89 (app. quintet, 2H, *J* = 7.2, CH₂), 1.56 (app. quintet, 2H, *J* = 6.3, CH₂), 1.55 (s, 3H), 1.44 (s, 9H), 1.43 (s, 9H), 1.31 (s, 3H) ppm; ¹³C NMR (100 MHz, CDCl₃) δ 154.7, 149.0, 145.9, 125.9, 124.4, 114.2, 94.1, 86.8 (d, *J* = 7.9), 85.1, 82.71 (d, *J* = 7.3), 82.69 (d, *J* = 7.2), 81.3, 66.4 (d, *J* = 6.3), 61.7, 44.5, 29.74 (d, 3C, *J* = 4.2), 29.72 (d, 3C, *J* = 4.3), 29.1, 27.1, 26.2, 25.2 ppm; ³¹P NMR (162 MHz, ¹H decoupled, CDCl₃) δ -10.4 ppm; HRMS (ESI⁺) calcd for C₂₅H₄₀N₄O₉P⁷⁹BrNa 673.1608 [(M + H)⁺], found 673.1584, calcd for C₂₅H₄₀N₄O₉P⁸¹BrNa 675.1588 [(M + H)⁺], found 675.1570.

N1-[2',3'-O-Isopropylidine-5'-O-(di-tert-butyl)phosphoryl-β-D-ribofuranosyl]-N9-(4-[(diphenylthio)phosphoryl]-hydroxybutyl)-8-bromohypoxanthine (22). Intermediate 21 (20 mg, 0.031 mmol) was coevaporated from pyridine (3 × 1 mL) and taken up in pyridine (0.5 mL). This solution was added to PSS (35 mg, 0.092 mmol) which had also been coevaporated from pyridine (3 × 1 mL). 5-Phenyl-1-H-tetrazole (13 mg, 0.092 mmol) and TPS-Cl (19 mg, 0.061 mmol) were added, and the solution was stirred at rt for 5 h. DCM and H₂O were added. The organic layer was separated and the aqueous layer washed with DCM (×2). The combined organic layer was washed with brine, dried (Na₂SO₄), and evaporated to dryness. The residue was purified by column chromatography on silica gel, eluting with PE/EtOAc (1:0 → 1:0 v/v) to afford the title compound (28 mg, 100%) as a white foam. *R*_f = 0.73 (DCM/acetone 1:1 v/v); ¹H NMR (400 MHz, CDCl₃) δ 8.04 (s, 1H, H-2), 7.52–7.49 (m, 4H), 7.36–7.30 (m, 6H) (10 × Ar-H), 5.97 (d, 1H, *J* = 1.8, H-1'), 5.07 (dd, 1H, *J* = 6.4, 1.8, H-2'), 4.98 (dd, 1H, *J* = 6.4, 3.9, H-3'), 4.40 (app. dd, 1H, *J* = 9.4, 5.2, H-4'), 4.25–4.17 (m, 4H, both H-5' and CH₂), 4.11 (t, 2H, *J* = 7.0, CH₂), 1.82 (app. quintet, 2H, *J* = 7.2, CH₂), 1.66 (app. quintet, 2H, *J* = 6.3, CH₂), 1.56 (s, 3H), 1.454 (s, 9H), 1.449 (s, 9H), 1.32 (s, 3H) ppm; ¹³C NMR (100 MHz, CDCl₃) δ 154.7, 149.0, 146.0, 135.2 (d, 4C, *J* = 5.2), 129.4 (d, 2C, *J* = 3.2), 129.3 (d, 4C, *J* = 2.5), 126.3 (d, 2C, *J* = 6.7), 125.8, 124.5, 114.3, 94.3, 86.8

(d, *J* = 7.9), 85.0, 82.8 (d, 2C, *J* = 7.3), 81.4, 67.0 (d, *J* = 8.7), 66.5 (d, *J* = 6.2), 43.9, 29.77 (d, 3C, *J* = 4.2), 29.74 (d, 3C, *J* = 4.2), 27.1, 27.0 (d, *J* = 6.7), 25.6, 25.2 ppm; ³¹P NMR (162 MHz, ¹H decoupled, CDCl₃) δ 49.0, -10.3 ppm; HRMS (ESI⁺) calcd for C₃₇H₄₉N₄O₁₀P₂S₂⁷⁹BrNa 937.1441 [(M + H)⁺], found 937.1447, calcd for C₃₇H₄₉N₄O₁₀P₂S₂⁸¹BrNa 939.1420 [(M + H)⁺], found 939.1440.

N1-[5'-O-Phosphoryl-β-D-ribofuranosyl]-N9-(4-[(diphenylthio)phosphoryl]hydroxybutyl)-8-bromo-hypoxanthine (23). Intermediate 22 (40 mg, 0.044 mmol) was stirred in 50% TFA (2 mL) at 0 °C for 4 h. All solvents were evaporated, and the residue was coevaporated with MeOH (×4). The residue was purified by column chromatography on silica gel, eluting with EtOAc/MeOH/H₂O (1:0:0 → 4:2:0 → 7:2:1 v/v/v) to afford the title compound (33 mg, 100%) as a colorless glass. *R*_f = 0.20 (EtOAc/MeOH/H₂O 7:2:1 v/v/v); ¹H NMR (500 MHz, MeOD) δ 8.59 (s, 1H, H-2), 7.43 (dd, 4H, *J* = 7.1, 0.7), 7.33–7.28 (m, 6H) (10 × ArH), 6.21 (d, 1H, *J* = 3.8, H-1'), 4.24 (d, 2H, *J* = 2.6, H-2' and H-3'), 4.16–4.07 (m, 7H, H-4', both H-5' and 2 × CH₂), 1.70 (app. quintet, 2H, *J* = 7.1, CH₂), 1.55 (app. quintet, 2H, *J* = 5.7, CH₂) ppm; ¹³C NMR (125 MHz, MeOD) δ 157.2, 150.6, 147.1, 136.6 (d, 4C, *J* = 5.3), 131.1 (d, 2C, *J* = 3.4), 130.7 (d, 4C, *J* = 2.5), 127.6, 127.0 (d, 2C, *J* = 6.8), 124.5, 89.8, 85.6 (d, *J* = 8.6), 77.1, 71.4, 69.2 (d, *J* = 8.9), 65.3 (d, *J* = 4.8), 45.2, 28.3 (d, *J* = 7.0), 26.8 ppm; ³¹P NMR (202 MHz, ¹H decoupled, MeOD) δ 50.8, 0.8 ppm; HRMS (ESI⁺) calcd for C₂₆H₂₈N₄O₁₀P₂S₂⁷⁹Br 760.9911 [(M - H)⁻], found 760.9878, calcd for C₂₆H₂₈N₄O₁₀P₂S₂⁸¹Br 762.9890 [(M - H)⁻], found 762.9915.

N1-[5'-O-Phosphoryl-β-D-ribofuranosyl]-N9-(4-[(diphenylthio)phosphoryl]hydroxybutyl)-8-bromo-hypoxanthine (24). Intermediate 23 (20 mg, 0.026 mmol) was taken up in dioxane/H₂O (1 mL, 1:1 v/v). NaOH (100 μL, 1 M) was added and the solution stirred for 30 min at rt before addition of HCl (100 μL, 1 M). The solution was diluted with H₂O and washed with hexane (×3) before evaporation of all solvents to give a colorless glass which was converted to the TEA salt as described below. ³¹P NMR (202 MHz, ¹H decoupled, D₂O) δ 15.6, 2.6 ppm; HRMS (ESI⁺) calcd for C₂₀H₂₄N₄O₁₁P₂S⁷⁹Br 668.9826 [(M - H)⁻], found 668.9853, calcd for C₂₀H₂₄N₄O₁₁P₂S⁸¹Br 670.9806 [(M - H)⁻], found 670.9863. Conversion to TEA salt: The Na⁺ salt was passed through prewashed Dowex H⁺ resin. Acidic fractions were neutralized with TEAB (2 mL, 1 M). All solvents were evaporated, and the residue was coevaporated with H₂O to remove excess buffer. The colorless glass obtained was used directly for cyclization.

N1-Cyclic-8-bromohypoxanthine-N9-hydroxybutyl Diposphate Ribose (8-Br-N9-butyl-cIDPR, 5). Intermediate 24 (0.026 mmol) was evaporated from pyridine (2 × 2 mL). The residue was taken up in pyridine (10 mL) and placed in a syringe. This solution was added over 15 h to a solution of iodine (70 mg, 0.30 mmol) and 3 Å molecular sieves (0.5 g) in pyridine (20 mL), in the dark. The solution was filtered through Celite, washed with H₂O. After addition of TEAB (2 mL) all solvents were evaporated, and the residue was partitioned between H₂O and CHCl₃. The aqueous layer was washed with CHCl₃ and evaporated to dryness. The residue was purified by semipreparative HPLC (1.1 cm × 25 cm C₁₈ column), eluting with acetonitrile/0.1 M TEAB (1:19 → 13:7 v/v) over 25 min. Fractions were analyzed by analytical HPLC and appropriate fractions collected and evaporated under vacuum to give the title compound (3.0 mg, 21% over two steps). UV (H₂O, pH 7), λ_{max} = 256 nm (ϵ = 19 900); ¹H NMR (500 MHz, D₂O) δ 8.81 (s, 1H, H-2), 6.08 (d, 1H, *J* = 1.8, H-1'), 4.43 (dd, 1H, *J* = 4.7, 1.8, H-2'), 4.38 (dd, 1H, *J* = 6.9, 4.7, H-3'), 4.35–4.19 (m, 4H), 4.17 (app. septet, 1H, *J* = 5.1, CH₂H), 4.11 (dd, 1H, *J* = 11.0, 3.9, H-5b'), 1.92–1.83 (m, 2H, CH₂H), 1.41–1.38 (m, 1H, CH₂H), 1.13–1.07 (m, 1H, CH₂H) ppm; ¹³C NMR (125 MHz, D₂O) δ 156.7, 150.1, 145.0, 127.7, 122.6, 91.1, 83.5 (d, *J* = 8.9), 75.2, 68.1, 65.2 (d, *J* = 6.0), 62.8 (d, *J* = 4.3), 42.9, 24.8 (d, *J* = 9.8), 23.7 ppm; ³¹P NMR (202 MHz, D₂O, ¹H-decoupled) δ -10.2 (d, *J* = 14.9 Hz), -11.4 (d, *J* = 14.9 Hz) ppm; HRMS (ESI⁺) calcd for C₁₄H₁₈N₄O₁₁P₂⁷⁹Br 558.9636 [(M - H)⁻], found 558.9627; calcd for C₁₄H₁₈N₄O₁₁P₂⁸¹Br 560.9616 [(M - H)⁻], found 560.9612.

N1-Cyclic Hypoxanthine-N9-hydroxybutyl Diposphate Ribose (N9-Butyl-cIDPR, 4). Analog 5 (7.0 mg, 0.0125 mmol) was

taken up in Milli-Q (3 mL), and NaHCO₃ (225 mg, 2.77 mmol) was added. When all material had dissolved, EtOH (1.5 mL) and then Pd/C (6 mg) were added and the solution was placed under an atmosphere of H₂. After 5 h stirring, the solution was filtered and all solvents evaporated. The residue was purified by semipreparative HPLC (1.1 cm × 25 cm C₁₈ column), eluting with MeCN/0.1 M TEAB (1:19 → 13:7 v/v) over 25 min. Fractions were analyzed by analytical HPLC and appropriate fractions collected and evaporated under vacuum to give the title compound (4.6 mg, 76%). UV (H₂O, pH 7), $\lambda_{\text{max}} = 252$ nm ($\epsilon = 11\,400$); ¹H NMR (500 MHz, D₂O) δ 8.79 (s, 1H, H-2), 8.03 (s, 1H, H-8), 6.10 (s, 1H, H-1'), 4.49 (d, 1H, J = 3.0, H-2'), 4.40 (app. t, 1H, J = 3.0, H-3'), 4.33–4.24 (m, 4H), 4.11 (dd, 1H, J = 11.8, 4.4, H-5a'), 4.05 (app septet, 1H, J = 5.2, CH₂H), 3.81 (app septet, 1H, J = 5.2, CH_bH), 1.96–1.84 (m, 2H, CH₂), 1.41–1.35 (m, 1H, CH_aH), 1.11–1.05 (m, 1H, CH_bH) ppm; ¹³C NMR (125 MHz, D₂O) δ 158.0, 148.9, 144.7, 142.3, 122.2, 91.1, 83.6 (d, J = 8.9), 75.2, 68.3, 65.1 (d, J = 5.9), 63.0 (d, J = 4.5), 42.3, 25.4, 25.0 (d, J = 9.5) ppm; ³¹P NMR (202 MHz, D₂O, ¹H-decoupled) δ -10.3 (d, J = 14.1), -11.2 (d, J = 14.2) ppm; HRMS (ESI⁻) calcd for C₁₄H₁₉N₄O₁₁P₂ 481.0531 [(M - H)⁻], found 481.0522.

N1-Cyclic-8-azidohypoxanthine-N9-hydroxybutyl Diposphate Ribose (8-N₃-N9-butyl-cIDPR, 6). Analog 5 (4.5 mg, 8.0 μmol) was converted to the free acid by addition of Milli-Q (5 mL) and stirring with Dowex 50WX8 (H⁺ form) for 30 min. The resin was removed by filtration, washed with Milli-Q and the combined filtrate evaporated. The residue was evaporated from dry DMF (4 × 2 mL), taken up in DMF (1 mL), and stirred under argon. TMSN₃ (50 μL, 0.43 mmol) was added and the resulting solution stirred at 70 °C in the dark for 16 h, after which ~65% conversion of the starting material to product was observed by HPLC ($\lambda = 255$ nm → $\lambda = 277$ nm). All solvent was evaporated and the resulting residue coevaporated with Milli-Q (2 × 5 mL). The residue was then taken up in Milli-Q (5 mL), filtered through cotton wool, and purified by semipreparative HPLC (1.1 cm × 25 cm C₁₈ column), eluting with acetonitrile/Milli-Q (1:19 → 13:7 v/v) over 25 min. Fractions were analyzed by analytical HPLC and appropriate fractions were collected and evaporated under vacuum to give the title compound (2.4 mg, 57%). UV (H₂O, pH 7), $\lambda_{\text{max}} = 252$ nm ($\epsilon = 12\,700$); ¹H NMR (500 MHz, D₂O) δ 8.75 (s, 1H, H-2), 6.08 (d, 1H, J = 1.9, H-1'), 4.46 (dd, 1H, J = 4.8, 1.9, H-2'), 4.39 (dd, 1H, J = 6.5, 4.8, H-3'), 4.33–4.30 (m, 2H, H-4', CHH), 4.12–4.05 (m, 3H, H-5'a, 2 × CHH), 4.00 (dt, 1H, J = 14.5, 5.2, H-5'b), 3.81 (app septet, 1H, J = 5.0, CHH), 1.81–1.76 (m, 2H, CH₂), 1.40–1.36 (m, 1H, CHH), 1.14–1.09 (m, 1H, CHH) ppm; ¹³C NMR (125 MHz, D₂O) 156.6, 149.0, 146.4, 144.2, 120.3, 91.2, 83.6 (d, J = 8.9), 75.2, 68.2, 65.1 (d, J = 6.5), 62.9 (d, J = 4.4), 40.7, 24.9 (d, J = 9.1), 23.5 ppm; ³¹P NMR (202 MHz, D₂O) -10.4 (d, J = 14.1), -11.4 (d, J = 14.1) ppm; HRMS (ESI⁻) found m/z [M - H]⁻ 522.0549; C₁₄H₁₈N₇O₁₁P₂ requires 522.0545.

N1-Cyclic-8-aminohypoxanthine-N9-hydroxybutyl Diposphate Ribose (8-NH₂-N9-butyl-cIDPR, 7). Analog 5 (4.5 mg, 8.0 μmol) was converted to the free acid by addition of Milli-Q (5 mL) and stirring with Dowex 50WX8 (H⁺ form) for 30 min. The resin was removed by filtration, washed with Milli-Q and the combined filtrate evaporated. The residue was evaporated from dry DMF (4 × 2 mL), taken up in DMF (1 mL), and stirred under argon. TMSN₃ (50 μL, 0.43 mmol) was added and the resulting solution stirred at 70 °C in the dark for 16 h, after which ~70% conversion of the starting material to product was observed by HPLC ($\lambda = 255$ nm → $\lambda = 277$ nm). All solvent was evaporated, and the resulting residue was taken up in TEAB (5 mL, 0.05 M). Dithiothreitol (12 mg, 0.08 mmol) was added and the solution stirred under an atmosphere of argon for 16 h. The crude material was directly purified by semipreparative HPLC (1.1 cm × 25 cm C₁₈ column), eluting with acetonitrile/0.1 M TEAB (1:19 → 13:7 v/v) over 25 min. Fractions were analyzed by analytical HPLC and appropriate fractions collected and evaporated under vacuum to give the title compound (2.7 mg, 68% over two steps). UV (H₂O, pH 7), $\lambda_{\text{max}} = 252$ nm ($\epsilon = 14\,700$); ¹H NMR (400 MHz, D₂O) δ 8.80 (s, 1H, H-2), 6.19 (d, 1H, J = 2.1, H-1'), 4.56 (dd, 1H, J = 4.7, 2.1, H-2'), 4.50 (dd, 1H, J = 6.4, 4.7, H-3'), 4.43–4.41 (m, 2H, H-4', CHH), 4.27–4.20 (m, 3H, H-5'a, 2 × CHH), 4.11 (ddd, 1H, J = 15.0, 5.3, 4.9,

H-5'b), 3.95 (app septet, 1H, J = 5.3, CHH), 2.00–1.85 (m, 2H, CH₂), 1.53–1.50 (m, 1H, CHH), 1.31–1.28 (m, 1H, CHH) ppm; ¹³C NMR (125 MHz, D₂O) 155.3, 152.2, 148.3, 143.2, 116.7, 91.1, 83.5 (d, J = 8.9), 75.2, 68.1, 65.1 (d, J = 5.6), 62.9 (d, J = 3.1), 39.7, 24.8 (d, J = 9.6), 22.5 ppm; ³¹P NMR (202 MHz, D₂O) -10.39 (br), -11.44 (br); HRMS (ESI⁻) found m/z [M - H]⁻ 496.0637; C₁₄H₂₀N₅O₁₁P₂ requires 496.0640.

Enzyme Assay for cADPR Hydrolysis. The inhibition of cADPR hydrolysis by various concentrations of analog (0–1 mM) was determined by incubating 1 μM cADPR with 1 μg/mL CD38 catalytic domain for 10 min at 20–24 °C in 25 mM sodium acetate, pH 4.5. The reaction was stopped by the addition of 150 mM HCl. The precipitated protein was filtered, and the pH was neutralized with Tris base. After the mixture was diluted 20-fold, the concentration of the unhydrolyzed cADPR present in the diluted reaction mixture was assayed by the fluorimetric cycling assay as described previously.⁵²

Modeling of the Butyl Compounds. The 2PGJ crystal structure of human CD38 with cIDPR was passed through the Protein Preparation Wizard in the Schrödinger software (<http://www.schrodinger.com/>). Four N9-butyl compounds, where the cIDPR “southern” ribose is replaced by a four carbon linker, were built using the Schrödinger software. The four compounds differed in the substituent at the 8-position: hydrogen, bromine, azido, or an amino group. The compounds were docked into the 2PGJ structure using GOLD.⁵⁸ The binding site was defined as a sphere of 5 Å radius centered on the centroid of the cIDPR ligand: the centroid of the docked ligand has to lie within this sphere. Each ligand was docked 25 times. The best ranked pose of each of the ligands was merged with the protein structure, and the resulting complex was passed through a minimization procedure using the Schrödinger software.

Crystallization, Diffraction Data Collection, and Structure Refinement. The human CD38 catalytic domain was expressed and purified as described previously.^{45,54} The protein was diluted to 10 mg/mL for crystallization trials. Crystals of wild type CD38 were obtained by the hanging droplet vapor diffusion method with the reservoir buffer in 0.1 M sodium acetate, pH 4.0, 15% PEG 10K, 0.2 M ammonium acetate, and 3% isopropanol. They were harvested and soaked in 0.1 M sodium acetate, pH 4.0, 15% PEG 10K, 16% ethylene glycerol, and 5 mM compound 7 for 1 h at 295 K and then flash-frozen in liquid nitrogen. The diffraction data were collected at 100 K on beamline BL17U at the Shanghai Synchrotron Radiation Facility and processed with HKL2000.⁵⁹ Molecular replacement was performed using the program Phaser⁶⁰ from the CCP4 suite,⁶¹ and the wild-type human CD38 (PDB code 1YH3) was used as the search model. The model was refined with Refmac⁶² and then cycled with manual building in Coot.⁶³ Hydrolyzed compound 7 was built into positive difference electron-density maps of the CD38 model after a few restrained refinement runs with the stereochemical restraints generated from the program PRODRG.⁶⁴ TLS refinement⁶⁵ was incorporated into the later stages of the refinement process. Solvents were added automatically in Coot and then manually inspected and modified. The final model was analyzed with MolProbity,⁶⁶ showing that 98% residues were in the Ramachandran favored region with only one residue (D202 in chain B) in the Ramachandran outlier region. Data collection and model refinement statistics are summarized in Supporting Information Table 1. The coordinates and structure factors are deposited in the Protein Data Bank with the code 4TMF.

HPLC Studies. The solution containing the CD38 catalytic domain was adjusted to the desired concentration using Tris-HCl buffer (20 mM, pH 8), and 50 μL therefrom was added to the inhibitor (0.05 μmol) in an Eppendorf tube at room temperature. At a given time point, a sample of 5 μL was removed and diluted with 95 μL of Milli-Q water. Then 10 μL of this sample was injected directly into the analytical HPLC system (see section General in Experimental Section), eluting at 1 mL/min with an isocratic ion-pair buffer: 0.17% (m/v) cetrimeide and 45% (v/v) phosphate buffer (pH 6.4) in MeOH.

■ ASSOCIATED CONTENT

Supporting Information

Figures S1–S3, crystallographic data collection, model refinement statistics, HPLC traces, and ^1H NMR and ^{13}C NMR spectra for all novel compounds. This material is available free of charge via the Internet at <http://pubs.acs.org>.

Accession Codes

The structure of the shCD38:7a complex has been deposited in the PDB with the code 4TMF.

■ AUTHOR INFORMATION

Corresponding Author

*Phone: ++44-1225-386639. Fax: ++44-1225-386114. E-mail: B.V.L.Potter@bath.ac.uk.

Notes

The authors declare no competing financial interest.

■ ACKNOWLEDGMENTS

We acknowledge Grants RCGAS 201105159001 (to R.G.), HK-GRF 766911 (to Q.H.), and HK-GRF HKU 785110M (to H.Z.). BVLP is a Wellcome Trust Senior Investigator (Grant 101010).

■ ABBREVIATIONS USED

ADPR, adenosine 5'-diphosphate ribose; ADPRC, adenosine 5'-diphosphate ribosyl cyclase; cADPR, cyclic adenosine 5'-diphosphoribose; cADPcR, cyclic adenosine 5'-diphosphate carbocyclic ribose; cIDPR, cyclic inosine 5'-diphosphoribose; NAADP, nicotinic acid adenine dinucleotide phosphate; NAD $^+$, nicotinamide adenosine 5'-dinucleotide; NADP, nicotinamide adenine dinucleotide phosphate; N9-butyl-cIDPR, cyclic-N9-butylhypoxanthine 5'-diphosphate ribose; shCD38, CD38 catalytic domain

■ ADDITIONAL NOTE

^aNote that for the N9-butyl analogs, the prime notation refers to the N1-ribose, in contrast to the natural products where the prime notation refers to the N9-ribose.

■ REFERENCES

- (1) Clapper, D. L.; Walseth, T. F.; Dargie, P. J.; Lee, H. C. Pyridine-nucleotide metabolites stimulate calcium release from sea-urchin egg microsomes desensitized to inositol trisphosphate. *J. Biol. Chem.* **1987**, *262*, 9561–9568.
- (2) Lee, H. C.; Aarhus, R.; Levitt, D. The crystal structure of cyclic ADP-ribose. *Nat. Struct. Biol.* **1994**, *1*, 143–144.
- (3) Lee, H. C. Multiplicity of Ca^{2+} messengers and Ca^{2+} stores: a perspective from cyclic ADP-ribose and NAADP. *Curr. Mol. Med.* **2004**, *4*, 227–237.
- (4) Guse, A. H. Biochemistry, biology, and pharmacology of cyclic adenosine diphosphoribose (cADPR). *Curr. Med. Chem.* **2004**, *11*, 847–855.
- (5) Potter, B. V. L.; Walseth, T. F. Medicinal chemistry and pharmacology of cyclic ADP-ribose. *Curr. Mol. Med.* **2004**, No. 4, 303–311.
- (6) Guse, A. H. Second messenger function and the structure-activity relationship of cyclic adenosine diphosphoribose (cADPR). *FEBS J.* **2005**, *272*, 4590–4597.
- (7) Zhao, Y. J.; Lam, C. M. C.; Lee, H. C. The membrane-bound enzyme CD38 exists in two opposing orientations. *Sci. Signaling* **2012**, *S*, ra67.
- (8) Perraud, A. L.; Fleig, A.; Dunn, C. A.; Bagley, L. A.; Launay, P.; Schmitz, C.; Stokes, A. J.; Zhu, Q. Q.; Bessman, M. J.; Penner, R.; Kinet, J. P.; Scharenberg, A. M. ADP-ribose gating of the calcium-permeable LTRPC2 channel revealed by Nudix motif homology. *Nature* **2001**, *411*, 595–599.
- (9) Kim, H.; Jacobson, E. L.; Jacobson, M. K. Synthesis and degradation of cyclic ADP-ribose by NAD glycohydrolases. *Science* **1993**, *261*, 1330–1333.
- (10) Howard, M.; Grimaldi, J.; Bazan, J.; Lund, F.; Santos-Argumedo, L.; Parkhouse, R.; Walseth, T.; Lee, H. Formation and hydrolysis of cyclic ADP-ribose catalyzed by lymphocyte antigen CD38. *Science* **1993**, *262*, 1056–1059.
- (11) Cosker, F.; Cheviron, N.; Yamasaki, M.; Menteyne, A.; Lund, F. E.; Moutin, M. J.; Galione, A.; Cancela, J. M. The ecto-enzyme CD38 is a nicotinic acid adenine dinucleotide phosphate (NAADP) synthase that couples receptor activation to Ca^{2+} mobilization from lysosomes in pancreatic acinar cells. *J. Biol. Chem.* **2010**, *285*, 38251–38259.
- (12) Savarino, A.; Bensi, T.; Chiocchetti, A.; Bottarel, F.; Mesturini, R.; Ferrero, E.; Calosso, L.; Deaglio, S.; Ortolan, E.; Buttò, S.; Cafaro, A.; Katada, T.; Ensoli, B.; Malavasi, F.; Dianzani, U. Human CD38 interferes with HIV-1 fusion through a sequence homologous to the V3 loop of the viral envelope glycoprotein gp120. *FASEB J.* **2003**, *17*, 461–463.
- (13) Malavasi, F.; Deaglio, S.; Damle, R.; Cutrona, G.; Ferrarini, M.; Chiorazzi, N. CD38 and chronic lymphocytic leukemia: a decade later. *Blood* **2011**, *118*, 3470–3478.
- (14) Aksoy, P.; White, T. A.; Thompson, M.; Chini, E. N. Regulation of intracellular levels of NAD: a novel role for CD38. *Biochem. Biophys. Res. Commun.* **2006**, *345*, 1386–1392.
- (15) Young, G. S.; Choleris, E.; Lund, F. E.; Kirkland, J. B. Decreased cADPR and increased NAD $^+$ in the *Cd38^{-/-}* mouse. *Biochem. Biophys. Res. Commun.* **2006**, *346*, 188–192.
- (16) Chini, E. N. CD38 as a regulator of cellular NAD: a novel potential pharmacological target for metabolic conditions. *Curr. Pharm. Des.* **2009**, *15*, 57–63.
- (17) Jin, D.; Liu, H. X.; Hirai, H.; Torashima, T.; Nagai, T.; Lopatina, O.; Shnayder, N. A.; Yamada, K.; Noda, M.; Seike, T.; Fujita, K.; Takasawa, S.; Yokoyama, S.; Koizumi, K.; Shiraishi, Y.; Tanaka, S.; Hashii, M.; Yoshihara, T.; Higashida, K.; Islam, M. S.; Yamada, N.; Hayashi, K.; Noguchi, N.; Kato, I.; Okamoto, H.; Matsushima, A.; Salmina, A.; Muneshue, T.; Shimizu, N.; Mochida, S.; Asano, M.; Higashida, H. CD38 is critical for social behaviour by regulating oxytocin secretion. *Nature* **2007**, *446*, 41–45.
- (18) Liu, Z.; Graeff, R. M.; Jin, H.; Zhang, L.; Zhang, L. Studies on CD38 inhibitors and their application to cADPR-mediated Ca^{2+} signaling. *Messenger* **2013**, *2*, 19–32.
- (19) Sauve, A. A.; Schramm, V. L. Mechanism-based inhibitors of CD38: a mammalian cyclic ADP-ribose synthetase. *Biochemistry* **2002**, *41*, 8455–8463.
- (20) Dong, M.; Si, Y. Q.; Sun, S. Y.; Pu, X. P.; Yang, Z. J.; Zhang, L. R.; Zhang, L. H.; Leung, F. P.; Lam, C. M. C.; Kwong, A. K. Y.; Yue, J. B.; Zhou, Y. Y.; Kriksunov, I. A.; Hao, Q.; Lee, H. C. Design, synthesis and biological characterization of novel inhibitors of CD38. *Org. Biomol. Chem.* **2011**, *9*, 3246–3257.
- (21) Wall, K. A.; Klis, M.; Kornet, J.; Coyle, D.; Amé, J. C.; Jacobson, M. K.; Slama, J. T. Inhibition of the intrinsic NAD $^+$ glycohydrolase activity of CD38 by carbocyclic NAD analogues. *Biochem. J.* **1998**, *335*, 631–636.
- (22) Kellenberger, E.; Kuhn, I.; Schuber, F.; Muller-Steffner, H. Flavonoids as inhibitors of human CD38. *Bioorg. Med. Chem. Lett.* **2011**, *21*, 3939–3942.
- (23) Zhou, Y.; Ting, K. Y.; Lam, C. M. C.; Kwong, A. K. Y.; Xia, J.; Jin, H.; Liu, Z.; Zhang, L.; Lee, H. C.; Zhang, L. Design, synthesis and biological evaluation of noncovalent inhibitors of human CD38 NADase. *ChemMedChem* **2012**, *7*, 223–228.
- (24) Sauve, A. A.; Deng, H. T.; Angeletti, R. H.; Schramm, V. L. A covalent intermediate in CD38 is responsible for ADP-ribosylation and cyclisation reactions. *J. Am. Chem. Soc.* **2000**, *122*, 7855–7859.
- (25) Ashamu, G. A.; Sethi, J. K.; Galione, A.; Potter, B. V. L. Roles for adenosine ribose hydroxyl groups in cyclic adenosine 5'-diphosphate ribose-mediated Ca^{2+} -release. *Biochemistry* **1997**, *36*, 9509–9517.

- (26) Guse, A. H.; Cakir-Kiefer, C.; Fukuoka, M.; Shuto, S.; Weber, K.; Bailey, V. C.; Matsuda, A.; Mayr, G. W.; Oppenheimer, N.; Schuber, F.; Potter, B. V. L. Novel hydrolysis-resistant analogues of cyclic ADP-ribose: modification of the "northern" ribose and calcium release activity. *Biochemistry* **2002**, *41*, 6744–6751.
- (27) Bailey, V. C.; Fortt, S. M.; Summerhill, R. J.; Galione, A.; Potter, B. V. L. Cyclic aristeromycin diphosphate ribose: a potent and poorly hydrolysable Ca^{2+} -mobilising mimic of cyclic adenosine diphosphate ribose. *FEBS Lett.* **1996**, *379*, 227–230.
- (28) Wagner, G. K.; Guse, A. H.; Potter, B. V. L. Rapid synthetic route toward structurally modified derivatives of cyclic adenosine 5'-diphosphate ribose. *J. Org. Chem.* **2005**, *70*, 4810–4819.
- (29) Wagner, G. K.; Black, S.; Guse, A. H.; Potter, B. V. L. First enzymatic synthesis of an N1-cyclised cADPR (cyclic ADP-ribose) analogue with a hypoxanthine partial structure: discovery of a membrane permeant cADPR agonist. *Chem. Commun.* **2003**, 1944–1945.
- (30) Kirchberger, T.; Moreau, C.; Wagner, G. K.; Fliegert, R.; Siebrands, C. C.; Nebel, M.; Schmid, F.; Harneit, A.; Odoardi, F.; Flugel, A.; Potter, B. V. L.; Guse, A. H. 8-Bromo-cyclic inosine diphosphoribose: towards a selective cyclic ADP-ribose agonist. *Biochem. J.* **2009**, *422*, 139–149.
- (31) Shuto, S.; Fukuoka, M.; Manikowsky, A.; Ueno, Y.; Nakano, T.; Kuroda, R.; Kuroda, H.; Matsuda, A. Total synthesis of cyclic ADP-carbocyclic ribose, a stable mimic of Ca^{2+} -mobilizing second messenger cyclic ADP-ribose. *J. Am. Chem. Soc.* **2001**, *123*, 8750–8759.
- (32) Shuto, S.; Shirato, M.; Sumita, Y.; Ueno, Y.; Matsuda, A. Synthesis of cyclic IDP-carbocyclic-ribose, a stable mimic of cyclic ADP-ribose. Significant facilitation of the intramolecular condensation reaction of N1-(carbocyclic-ribosyl)inosine 5',6"-diphosphate derivatives by an 8-bromo-substitution at the hypoxanthine moiety. *J. Org. Chem.* **1998**, *63*, 1986–1994.
- (33) Fukuoka, M.; Shuto, S.; Minakawa, N.; Ueno, Y.; Matsuda, A. An efficient synthesis of cyclic IDP and cyclic 8-bromo-IDP-carbocyclic-riboses using a modified Hata condensation method to form an intramolecular pyrophosphate linkage as a key step. An entry to a general method for the chemical synthesis of cyclic ADP-ribose analogues. *J. Org. Chem.* **2000**, *65*, 5238–5248.
- (34) Gu, X.; Yang, Z.; Zhang, L.; Kunerth, S.; Fliegert, R.; Weber, K.; Guse, A. H. Synthesis and biological evaluation of novel membrane-permeant cyclic ADP-ribose mimics: N1-[5"-O-phosphorylethoxy]-methyl]-5'-O-phosphorylinosine-5',5"-cyclicpyrophosphate (cIDPRE) and 8-substituted derivatives. *J. Med. Chem.* **2004**, *47*, 5674–5682.
- (35) Guse, A. H.; Gu, X. F.; Zhang, L. R.; Weber, K.; Kramer, E.; Yang, Z. J.; Jin, H. W.; Li, Q.; Carrier, L.; Zhang, L. H. A minimal structural analogue of cyclic ADP-ribose: synthesis and calcium release activity in mammalian cells. *J. Biol. Chem.* **2005**, *280*, 15952–15959.
- (36) Huang, L. J.; Zhao, Y. Y.; Yuan, L.; Min, J. M.; Zhang, L. H. Syntheses and calcium-mobilizing evaluations of N1-glycosyl-substituted stable mimics of cyclic ADP-ribose. *J. Med. Chem.* **2002**, *45*, 5340–5352.
- (37) Swarbrick, J. M.; Potter, B. V. L. Total Synthesis of a cyclic adenosine 5'-diphosphate ribose receptor agonist. *J. Org. Chem.* **2012**, *77*, 4191–4197.
- (38) Graeff, R. M.; Walseth, T. F.; Hill, H. K.; Lee, H. C. Fluorescent analogs of cyclic ADP-ribose: synthesis, spectral characterization, and use. *Biochemistry* **1996**, *35*, 379–386.
- (39) Graeff, R.; Liu, Q.; Kriksunov, I. A.; Kotaka, M.; Oppenheimer, N.; Hao, Q.; Lee, H. C. Mechanism of cyclizing NAD to cyclic ADP-ribose by ADP-ribosyl cyclase and CD38. *J. Biol. Chem.* **2009**, *284*, 27629–27636.
- (40) Graeff, R.; Liu, Q.; Kriksunov, I. A.; Hao, Q.; Lee, H. C. Acidic residues at the active sites of CD38 and ADP-ribosyl cyclase determine nicotinic acid adenine dinucleotide phosphate (NAADP) synthesis and hydrolysis activities. *J. Biol. Chem.* **2006**, *281*, 28951–28957.
- (41) Liu, Q.; Kriksunov, I. A.; Graeff, R.; Munshi, C.; Lee, H. C.; Hao, Q. Crystal structure of human CD38 extracellular domain. *Structure* **2005**, *13*, 1331–1339.
- (42) Liu, Q.; Kriksunov, I. A.; Moreau, C.; Graeff, R.; Potter, B. V. L.; Lee, H. C.; Hao, Q. Catalysis associated conformational changes revealed by human CD38 complexed with a non-hydrolysable substrate analog. *J. Biol. Chem.* **2007**, *282*, 24825–24832.
- (43) Moreau, C.; Liu, Q.; Graeff, R.; Wagner, G. K.; Thomas, M. P.; Swarbrick, J. M.; Shuto, S.; Lee, H. C.; Hao, Q.; Potter, B. V. L. CD38 structure-based inhibitor design using the N1-cyclic inosine 5'-diphosphate ribose template. *PLoS One* **2013**, *8*, e66247.
- (44) Graeff, R. M.; Munshi, C.; Aarhus, R.; Johns, M.; Lee, H. C. A single residue at the active site of CD38 determines its NAD cyclizing and hydrolyzing activities. *J. Biol. Chem.* **2001**, *276*, 12169–12173.
- (45) Munshi, C.; Aarhus, R.; Graeff, R.; Walseth, T. F.; Levitt, D.; Lee, H. C. Identification of the enzymatic active site of CD38 by site-directed mutagenesis. *J. Biol. Chem.* **2000**, *275*, 21566–21571.
- (46) Kuhn, I.; Kellenberger, E.; Cakir-Kiefer, C.; Muller-Steffner, H.; Schuber, F. Probing the catalytic mechanism of bovine CD38/NAD⁺ glycohydrolase by site directed mutagenesis of key active site residues. *Biochim. Biophys. Acta, Proteins Proteomics* **2014**, *1844*, 1317–1331.
- (47) Moreau, C.; Woodman, T. J.; Potter, B. V. L. Unusual entry to the novel 8-halo-N1-ribosyl hypoxanthine system by degradation of a cyclic adenosine 5'-diphosphate ribose analogue. *Chem. Commun.* **2006**, 1127–1129.
- (48) Galeone, A.; Mayol, L.; Oliviero, G.; Piccialli, G.; Varra, M. Synthesis of a novel N1-carbocyclic, N9 butyl analogue of cyclic ADP-ribose (cADPR). *Tetrahedron* **2002**, *58*, 363–368.
- (49) Volpini, R.; Mishra, R. C.; Kachare, D. D.; Ben, D. D.; Lambertucci, C.; Antonini, I.; Vittori, S.; Marucci, G.; Sokolova, E.; Nistri, A.; Cristalli, G. Adenine-based acyclic nucleotides as novel P2X3 receptor ligands. *J. Med. Chem.* **2009**, *52*, 4596–4603.
- (50) Laufer, S. A.; Domezey, D. M.; Scior, T. R. F.; Albrecht, W.; Hauser, D. R. J. Synthesis and biological testing of purine derivatives as potential ATP-competitive kinase inhibitors. *J. Med. Chem.* **2005**, *48*, 710–722.
- (51) Nolsoe, J. M. J.; Gundersen, L.-L.; Rise, F. Synthesis of 8-halopurines by reaction of lithiated purines with appropriate halogen donors. *Synth. Commun.* **1998**, *28*, 4303–4315.
- (52) Graeff, R. M.; Lee, H. C. A novel cycling assay for cellular cADP-ribose with nanomolar sensitivity. *Biochem. J.* **2002**, *361*, 379–384.
- (53) Liu, Q.; Kriksunov, I. A.; Graeff, R.; Munshi, C.; Lee, H. C.; Hao, Q. Structural basis for the mechanistic understanding of human CD38-controlled multiple catalysis. *J. Biol. Chem.* **2006**, *281*, 32861–32869.
- (54) Zhang, H.; Graeff, R.; Lee, H. C.; Hao, Q. Crystal structures of human CD38 in complex with NAADP and ADPRP. *Messenger* **2013**, *2*, 44–53.
- (55) Sauve, A. A.; Munshi, C.; Lee, H. C.; Schramm, V. L. The reaction mechanism for CD38. A single intermediate is responsible for cyclization, hydrolysis, and base-exchange chemistries. *Biochemistry* **1998**, *37*, 13239–13249.
- (56) Kim, H.; Jacobson, E. L.; Jacobson, M. K. Position of cyclization in cyclic ADP-ribose. *Biochem. Biophys. Res. Commun.* **1993**, *194*, 1143–1147.
- (57) Ames, B. N.; Dubin, D. T. The role of polyamines in the neutralization of bacteriophage deoxyribonucleic acid. *J. Biol. Chem.* **1960**, *235*, 769–775.
- (58) Jones, G.; Willett, P.; Glen, R. C.; Leach, A. R.; Taylor, R. Development and validation of a genetic algorithm for flexible docking. *J. Mol. Biol.* **1997**, *267*, 727–748.
- (59) Otwinowski, Z.; Minor, W. Processing of X-ray diffraction data collected in oscillation mode. *Methods Enzymol.* **1997**, 307–325.
- (60) McCoy, A.; Grosse-Kunstleve, R.; Adams, P.; Winn, M.; Storoni, L.; Read, R. Phaser crystallographic software. *J. Appl. Crystallogr.* **2007**, *40*, 658–674.
- (61) Collaborative Computational Project, Number 4. The CCP4 suite: programs for protein crystallography. *Acta Crystallogr., Sect. D: Biol. Crystallogr.* **1994**, *50*, 760–763.

- (62) Murshudov, G.; Vagin, A.; Dodson, E. Refinement of macromolecular structures by the maximum-likelihood method. *Acta Crystallogr., Sect. D: Biol. Crystallogr.* **1997**, *53*, 240–255.
- (63) Emsley, P.; Lohkamp, B.; Scott, W. G.; Cowtan, K. Features and development of Coot. *Acta Crystallogr., Sect. D: Biol. Crystallogr.* **2010**, *66*, 486–501.
- (64) Schuttelkopf, A.; Van Aalten, D. PRODRG: a tool for high-throughput crystallography of protein–ligand complexes. *Acta Crystallogr., Sect. D: Biol. Crystallogr.* **2004**, *60*, 1355–1363.
- (65) Painter, J.; Merritt, E. TLSMD Web server for the generation of multi-group TLS models. *J. Appl. Crystallogr.* **2006**, *39*, 109–111.
- (66) Chen, V. B.; Arendall, W. B., 3rd; Headd, J. J.; Keedy, D. A.; Immormino, R. M.; Kapral, G. J.; Murray, L. W.; Richardson, J. S.; Richardson, D. C. MolProbity: all-atom structure validation for macromolecular crystallography. *Acta Crystallogr., Sect. D: Biol. Crystallogr.* **2010**, *66*, 12–21.